Journal of Mathematical Biology manuscript No.
(will be inserted by the editor)

Fractional Cable Equation Models for Anomalous Electrodiffusion in Nerve Cells: Infinite Domain Solutions

T.A.M. Langlands · B.I. Henry · S.L. Wearne

Received: date / Accepted: date

Abstract We introduce fractional Nernst-Planck equations and derive fractional cable equations as macroscopic models for electrodiffusion of ions in nerve cells when molecular diffusion is anomalous subdiffusion due to binding, crowding or trapping. The anomalous subdiffusion is modelled by replacing diffusion constants with time dependent operators parameterized by fractional order exponents. Solutions are obtained as functions of the scaling parameters for infinite cables and semi-infinite cables with instantaneous current injections. Voltage attenuation along dendrites in response to alpha function synaptic inputs is computed. Action potential firing rates are also derived based on simple integrate and fire versions of the models. Our results show that electrotonic properties and firing rates of nerve cells are altered by anomalous subdiffusion in these models. We have suggested electrophysiological experiments to calibrate and validate the models.

Keywords Dendrite · Cable equation · Anomalous diffusion · Fractional derivative

PACS 87.15.Vv · 87.19.La · 05.60.-k · 05.40.Fb

1 Introduction

The core conductor concept and associated cable equation provide a fundamental macroscopic basis for understanding electrophysiological behaviour in neuronal processes such as

T.A.M. Langlands · B.I. Henry
Department of Applied Mathematics,
School of Mathematics and Statistics,
University of New South Wales,
Sydney NSW 2052, Australia.
E-mail: B.Henry@unsw.edu.au

S.L. Wearne
Laboratory for Biomathematical Sciences,
Department of Neuroscience,
Mount Sinai School of Medicine,
New York, New York. 10029-6574.
E-mail: susan.wearne@mssm.edu

axons, dendrites, and dendritic trees [29,30]. The cable equation models spatio-temporal dynamics of the membrane potential along the axial direction of an approximately cylindrical segment of a nerve cell. This equation can be motivated phenomenologically by representing the electrical properties of the cell membrane as a contiguous network of circuits composed of passive resistors and capacitors in parallel [30]. A more fundamental motivation can be obtained from the Nernst-Planck equation for electrodiffusion of ions in an axially symmetric cylindrical geometry [28]. Here the Nernst-Planck equation provides a macroscopic approximation for the complicated microscopic motions of ions in nerve cells. The random Brownian motion of the ions, as well as the drift of ions due to the electric field of the membrane potential, is captured in this approximation. However in addition to these motions, ions can be trapped [32,33], buffered [10], or crowded [1,13] when diffusing in the cytoplasm, and obstructed by gating [18,12] or binding when diffusing through ion channels across the membrane. On macroscopic scales these obstacles slow the diffusive motion of the ions relative to free diffusion in aqueous media (see also [34–36,50]). Retarded diffusion of ions has been reported across ion channels [9] as well as along nerve cell membranes (through the cytoplasm) [33]. In applications of the Poisson Nernst-Planck theory for ionic motion through open channels this retarded motion can be incorporated using a spatially dependent diffusivity parameter that is typically one or more orders of magnitude lower than the free diffusivity [25,9].

A recent study [33] has found that the diffusion of molecules through the cytoplasm of Purkinje cell dendrites is slowed at the macroscopic scale, primarily through temporary trapping by dendritic spines, and also to a lesser extent through macromolecular crowding or binding [38,54]. An important finding of this study was that the diffusive spatial variance evolves as a sub-linear power law in time. This is a key signature of anomalous subdiffusion. Moreover it was found that the diffusion became more anomalous with increasing spine density [33]. Anomalous subdiffusion has also been reported in numerous other biological studies [8,39–41,5,1,31]. The above considerations provide clear motivation for attempting to develop new cable equation models for nerve cells that incorporate the possibility of anomalously slow electrodiffusion of ions.

Anomalous subdiffusion can be modelled at the macroscopic level through a modified diffusion equation

$$\frac{\partial C}{\partial t} = \mathscr{D}(\gamma,t)\nabla^2 C \tag{1}$$

in which $\mathscr{D}(\gamma,t)$ is a time dependent operator parameterized by a scaling exponent γ, in the range $0 < \gamma \leq 1$; the case $\gamma = 1$ corresponds to standard diffusion. Different models for the time dependent operator have been proposed that result in the power law diffusive spatial variance that is characteristic of anomalous subdiffusion. In order to differentiate between model dependent peculiarities and the general effects of anomalous diffusion on electrotonic properties, in the following we have considered two different models for this operator:
Model I [53,21]

$$\mathscr{D}_I(\gamma,t) = D(\gamma)\gamma t^{\gamma-1}; \tag{2}$$

Model II [24]

$$\mathscr{D}_{II}(\gamma,t) = D(\gamma)\frac{\partial^{1-\gamma}}{\partial t^{1-\gamma}}; \tag{3}$$

where $D(\gamma)$ is a generalized diffusion coefficient with units of $m^2 s^{-\gamma}$ and $\frac{\partial^{1-\gamma}}{\partial t^{1-\gamma}}$ is the Riemann-Liouville fractional derivative operator of order $1-\gamma$ defined by

$$\frac{\partial^{1-\gamma}}{\partial t^{1-\gamma}} Y(t) = \frac{1}{\Gamma(\gamma)} \frac{\partial}{\partial t} \int_0^t \frac{Y(t')}{(t-t')^{1-\gamma}} dt'. \tag{4}$$

While both models predict the same power law diffusive spatial variance, the physical development of the models has been different. Model I has been derived from a Langevin equation with a friction memory kernel and power law correlated noise [51–53] whereas Model II has been derived from Continuous Time Random Walks (CTRW) governed by a Gaussian step length density, but a power law waiting time density [24,17]. The origin of the power law behaviours in the above is usually associated with trapping or molecular crowding. For example a power law waiting time density is generic for random walks amid a sea of traps with an exponential distribution of trap binding energies $\rho(E) = \frac{1}{E_0} e^{-E/E_0}$ and thermally activated trapping times $\tau = e^{E/k_B T}$ [37]. An exponential distribution of trap binding energies can arise as the most probable distribution of a fixed amount of energy among a fixed number of traps. At the macroscopic level, a phenomenological derivation of the fractional diffusion equation corresponding to each model is possible by combining the standard continuity equation

$$\frac{\partial C}{\partial t} = -\nabla \cdot q \tag{5}$$

with a fractional Fick's law for the flux as follows:

$$q = -\mathscr{D}(\gamma, t) \nabla C. \tag{6}$$

where $\mathscr{D}(\gamma, t)$ is defined by (2) or (3).

The microscopic motion of ions in nerve cells is usually modelled as Fickian diffusion with drift; the latter due to the electric field of the cell membrane potential. The membrane electrical potential is produced by a capacitive separation of charge densities inside and outside the cell membrane. The total flux of the kth ionic species, q_k, in the standard Nernst-Planck theory is given by

$$q_k = -D_k \nabla C_k - \frac{z_k F}{RT} D_k C_k \nabla V_m. \tag{7}$$

In this equation, C_k is the concentration of the kth ionic species, F is the Faraday constant, R is the universal gas constant, T is the temperature and V_m is the membrane potential. A possible generalization of the flux, to incorporate anomalous diffusion, is to replace the species dependent diffusion constant D_k with a species dependent time dependent operator, $\mathscr{D}_k(\gamma_k, t)$, i.e.,

$$q_k = -\mathscr{D}_k(\gamma_k, t) \nabla C_k - \frac{z_k F}{RT} \mathscr{D}_k(\gamma_k, t) C_k \nabla V_m. \tag{8}$$

The subscript k on the scaling exponent allows the possibility of species dependent anomalous scaling. The resultant macroscopic electrodiffusion equation found by combining the standard continuity equation, (5) with the fractional Nernst-Planck flux, (8) is then given by

$$\frac{\partial C_k}{\partial t} = \mathscr{D}_k(\gamma_k, t) \nabla^2 C_k + \nabla \cdot \left(\frac{z_k F}{RT} \mathscr{D}_k(\gamma_k, t) C_k \nabla V_m \right) \tag{9}$$

where $\mathscr{D}_k(\gamma_k, t)$ is defined by (2) or (3).

At present we do not have a derivation for the fractional Nernst-Planck equation proposed in (9) from a more fundamental basis, such as biased continuous time random walks, however it is worthwhile considering some of the recent literature in this area. The fractional diffusion equation defined by (1) and (3), has been extended within the framework of continuous time random walks CTRWs, and a generalized master equation GME, to include external force fields [3,24,44], reactions [17,45,15,20], finite propagation velocities [6] and ageing [2]. In the case of anomalous subdiffusion with time independent external force fields a fractional Fokker-Planck equation has been derived from a GME [23] and from CTRWs [3,24]. In the case of anomalous subdiffusion with space independent external fields a fractional dispersal equation has been derived from a GME [44]. However these derivations do not extend to the more general case of anomalous subdiffusion in an external force field $f(x,t)$ that varies in both time and space [14]. In this more general case two models that have been considered are [43,48]

$$\frac{\partial C}{\partial t} = \frac{\partial^{1-\gamma}}{\partial t^{1-\gamma}} D_\gamma \nabla^2 C - \frac{\partial^{1-\gamma}}{\partial t^{1-\gamma}} \nabla \left(\frac{1}{\eta_\gamma} f(x,t) C(x,t) \right) \tag{10}$$

and [14]

$$\frac{\partial C}{\partial t} = \frac{\partial^{1-\gamma}}{\partial t^{1-\gamma}} D_\gamma \nabla^2 C - \nabla \left(\frac{1}{\eta_\gamma} f(x,t) \frac{\partial^{1-\gamma}}{\partial t^{1-\gamma}} C(x,t) \right) \tag{11}$$

where η_γ is a generalized friction coefficient with dimensions of $s^{\gamma-2}$. The two coefficients D_γ and η_γ can be related through a generalized Einstein-Stokes relation [23,24,43]. If the force is independent of time then the two formulations in (10) and (11) are equivalent. However if the force is time dependent then in (10) the force field is driven by the same time dependent operator that affects variations in the time dependent ionic concentrations, whereas in (11) this is not the case. In the case of a purely external force it has been argued that the temporal subordination in (10) is not appropriate [14,55]. The fractional Nernst-Planck equation, (9), has the same form as (10) but the electric field force, $-\nabla V_m$, in this case is not an external force, rather it arises from the membrane potential which is itself a function of the ionic concentrations.

In a recent letter [16] we considered the fractional Nernst-Planck equation, (9), as our starting point for modelling anomalous electrodiffusion in spiny dendrites. Related fractional cable equation models were derived and some model predictions were obtained for postsynpatic potentials propagating along (infinite length) dendrites. In this paper we provide more complete details on the derivation of the fractional cable models and we derive solutions for infinite and semi-infinite fractional cables with no current injections and with instantaneous current injections. Different boundary conditions have been considered in the semi-infinite cables. Solutions for infinite cables with alpha function synaptic inputs are also derived and used to infer voltage attenuation along dendrites with anomalous electrodiffusion. Results for firing rates are obtained using simple integrate and fire versions of the models for a membrane patch with constant current input.

The remainder of this paper is organized as follows. In section 2 we derive fractional cable equations from the generalized fractional Nernst-Planck equation, (9) . In section 3 we compare infinite domain fundamental solutions for each of the models. In section 4 we derive results for the postsynaptic potential in response to different input functions. In section 5 we describe semi-infinite domain solutions for different boundary conditions. In section 6 we derive and compare results for firing rates based on simple integrate and fire versions of the models. In section 7 we describe voltage attenuation measurements and voltage patch recordings that could be used to calibrate and validate the models. We conclude with a short discussion in section 8.

2 Fractional Cable Equation Models

Our approach for deriving fractional cable equations from fractional Nernst-Planck equations follows that of Qian and Sejnowski [28] for the standard cable equation. We consider a nerve cell segment with diameter d much smaller than length ℓ and integrate (9) in axially symmetric cylindrical coordinates over the circular cross-section of the neuron, with zero flux of ions at the centre. This results in

$$\frac{\partial C_k}{\partial t} = \mathscr{D}_k^\star(\gamma_k,t)\left\{D_k(\gamma_k)\frac{\partial^2 C_k}{\partial x^2} + \frac{z_k F}{RT}\frac{\partial}{\partial x}\left(D_k(\gamma_k)C_k\frac{\partial V_m}{\partial x}\right)\right\} - \frac{4}{d}J_k\Big|_{r=\frac{d}{2}} \tag{12}$$

where x is the longitudinal coordinate, r is the radial coordinate, J_k denotes the radial flux of ionic species k across the membrane and

$$\mathscr{D}_k^\star(\gamma_k,t) = \mathscr{D}_k(\gamma_k,t)/D_k(\gamma). \tag{13}$$

In standard cable theory for nerve cells the membrane potential is taken to be [49]

$$V_m(x,t) = V_{rest} + \frac{Fd}{4c_m}\sum_k z_k\left(C_k(x,t) - C_{k,rest}\right) \tag{14}$$

where V_{rest} is the resting membrane potential, c_m is the membrane capacitance per unit area of membrane and $C_{k,rest}$ is the resting concentration of the k^{th} ionic species. We also follow the standard assumption that the axial ionic concentration gradients are small ($\partial C_k/\partial x \approx 0$), but the prefactor $\frac{Fd}{4c_m}$ is large ($\partial V_m/\partial x \ncong 0$) [28]. In addition we assume that the trapping effects due to the geometry of spines are similar for different species of mobile ions ($\gamma_k \approx \gamma$). Using these results in (12) we obtain

$$c_m\frac{\partial V_m}{\partial t} = \mathscr{D}^\star(\gamma,t)\left(\frac{d}{4r_L}\frac{\partial^2 V_m}{\partial x^2}\right) - i_m + i_e \tag{15}$$

where

$$\frac{1}{r_L} = \frac{F^2}{RT}\sum_k z_k^2 D_k(\gamma)C_k, \tag{16}$$

defines a modified longitudinal resistivity $r_L(\gamma)$ with units of $\Omega m s^{\gamma-1}$, i_m is the total ionic transmembrane current per unit area defined by

$$i_m = \sum_k z_k F J_k, \tag{17}$$

and i_e has been included as an external current per unit surface area. Note that even though the concentration gradients have been assumed to be small, the residual effects of ionic diffusion are still manifest in the electrophysiological properties of the fractional cable equation through the dependence of longitudinal resistivity, $r_L(\gamma)$, on the diffusivity parameters γ and $D_k(\gamma)$, as in (16). The dependence of r_L on ionic diffusivity also occurs in the standard cable equation, but in the fractional cable equation the additional dependence on the scaling parameter allows for greater impact of the diffusion.

As an alternative to the physical derivation from the fractional Nernst-Planck equation, the fractional cable equation, (15), can be obtained phenomenologically by combining the standard current continuity equation

$$c_m\frac{\partial V_m}{\partial t} = -\frac{d}{4}\frac{\partial i_L}{\partial x} - i_m + i_e \tag{18}$$

with the longitudinal current density, i_L, described by a fractional variant of Ohm's Law,

$$i_L = -\mathscr{D}^*(\gamma,t)\frac{1}{r_L(\gamma)}\frac{\partial V_m}{\partial x}. \tag{19}$$

Allowing for a similar fractional flux for the ionic transmembrane current we write

$$i_m = \alpha(\kappa)\mathscr{D}^*(\kappa,t)\frac{V_m - V_{rest}}{r_m} \tag{20}$$

where κ is the exponent characterizing the anomalous flux across the membrane and $\alpha(\kappa)$ is an additional parameter with units of $s^{1-\kappa}$. In steady state conditions it is to be expected that the two exponents γ and κ are equal. It is possible to absorb $\alpha(\kappa)$ into a modified specific membrane resistance $r_m(\kappa) = r_m/\alpha(\kappa)$, identifying $\alpha(\kappa)$ as the effect of anomalous flux across the channels on the specific membrane resistance, and $\alpha(1) = 1$. The fractional order operator $\mathscr{D}^*(\kappa,t)$ would also apply to any external current i_e carried by ions traversing the membrane. ations (19) and (20) can be interpreted as either an aged linear response [42] or a retarded linear response [43], if $\mathscr{D}^*(\kappa,t)$ is the renormalized form of (2) or (3) respectively. A similar generalization of Fick's Law has been proposed in a phenomenological derivation of the fractional diffusion equation [56] and a retarded linear stress-strain response involving fractional derivatives has been proposed for viscoelastic materials [19].

Equations (15) and (20) can be combined to arrive at the linear fractional cable equations:

Model I

$$r_m c_m \frac{\partial V_I}{\partial t} = \frac{dr_m}{4r_L(\gamma)}\gamma t^{\gamma-1}\left(\frac{\partial^2 V_I}{\partial x^2}\right) - \alpha(\kappa)\kappa t^{\kappa-1}(V_I - r_m i_e), \tag{21}$$

Model II

$$r_m c_m \frac{\partial V_{II}}{\partial t} = \frac{dr_m}{4r_L(\gamma)}\frac{\partial^{1-\gamma}}{\partial t^{1-\gamma}}\left(\frac{\partial^2 V_{II}}{\partial x^2}\right) - \alpha(\kappa)\frac{\partial^{1-\kappa}}{\partial t^{1-\kappa}}(V_{II} - r_m i_e), \tag{22}$$

where $V = V_m - V_{rest}$ and the subscripts I and II are used to differentiate the two anomalous diffusion models. There is no loss of generality in having the same fractional temporal operator acting on both the potential and the external current terms since the external current could be defined to compensate this. In the case $\gamma = \kappa = 1$ both cable equations reduce to the standard cable equation

$$r_m c_m \frac{\partial V}{\partial t} = \frac{dr_m}{4r_L}\frac{\partial^2 V}{\partial x^2} - V + r_m i_e.$$

It is interesting to note that the linear fractional cable equation for Model I can be obtained by starting with a different fractional Nernst-Planck equation of the form

$$\frac{\partial C_k}{\partial t} = \mathscr{D}_k(\gamma_k,t)\nabla^2 C_k + \nabla\cdot\left(\frac{z_k F}{RT}\nabla V_m \mathscr{D}_k(\gamma_k,t)C_k\right) \tag{23}$$

but with $\mathscr{D}_k(\gamma_k,t)$ given by Model II. Thus the linear fractional cable equation in Model I can be obtained from the fractional fokker-planck equation, (10), with $f(x,t) = -\frac{\partial V_m}{\partial x}$ and $\mathscr{D}_k(\gamma_k,t) = D(\gamma)\gamma t^{\gamma-1}$ or from the fractional dispersal equation , (11), with $f(x,t) = -\frac{\partial V_m}{\partial x}$ and $\mathscr{D}_k(\gamma_k,t) = D(\gamma)\frac{\partial^{1-\gamma}}{\partial t^{1-\gamma}}$.

In a recent letter [16] we presented fundamental solutions of the linear fractional cable equations, (21), (22) on an infinite domain in the special case where $\gamma = \kappa$. In Model I these solutions are time retarded solutions of the standard cable equation and in Model II the

solutions are subordinated to solutions of the standard cable equation through a Levy stable law as shown in Appendix A. Here we present more general solutions (including $\gamma \neq \kappa$) for both infinite and semi-infinite domains. The analysis is facilitated by considering the dimensionless forms, of (21) and (22):
Model I

$$\frac{\partial V_I}{\partial T} = \gamma T^{\gamma-1} \frac{\partial^2 V_I}{\partial X^2} - \mu^2 \kappa T^{\kappa-1} \left(V_I - i_e r_m\right), \tag{24}$$

Model II

$$\frac{\partial V_{II}}{\partial T} = \frac{\partial^{1-\gamma}}{\partial T^{1-\gamma}} \frac{\partial^2 V_{II}}{\partial X^2} - \mu^2 \frac{\partial^{1-\kappa}}{\partial T^{1-\kappa}} \left(V_{II} - i_e r_m\right), \tag{25}$$

where

$$T = \frac{t}{\tau_m} \tag{26}$$

is the dimensionless time variable,

$$X = x \tau_m^{\frac{1-\gamma}{2}} / \sqrt{\frac{dr_m}{4r_L}} \tag{27}$$

is the dimensionless space variable, and

$$\mu^2 = \alpha(\kappa) \tau_m^{\kappa-1} \tag{28}$$

is a dimensionless function of κ.

It is important to note that solutions to the (fractional) cable equations may change in sign whereas solutions of (fractional) diffusion equations define probability densities which must remain positive. Physically, the solution of the cable equation is a membrane potential whereas the solution of a diffusion equation is a concentration. The two are related through (14) which shows how the potential can change sign whilst the concentrations remain positive.

3 Infinite Domain Solutions

3.1 Infinite Domain – Model I

In this section we derive the fundamental Green's solution, $G(X,T)$, for (24) in the infinite domain, with initial condition $V(X,0) = \delta(X)$ and no external current. This solution can be found readily by multiplying (24) by the integrating factor $e^{\mu^2 T^\kappa}$ and then introducing a change of variables

$$W(X,S) = e^{\mu^2 T^\kappa} V(X,T) \tag{29}$$

with

$$S = T^\gamma. \tag{30}$$

The equation describing the evolution of $W(X,S)$ is the standard diffusion equation

$$\frac{\partial W}{\partial S} = \frac{\partial^2 W}{\partial X^2} \tag{31}$$

with fundamental solution

$$G^*(X,S) = \frac{1}{\sqrt{4\pi S}} \exp\left(-\frac{X^2}{4S}\right) \tag{32}$$

and hence

$$G(X,T) = \frac{1}{\sqrt{4\pi T^{\gamma}}} e^{-\frac{X^2}{4T^{\gamma}} - \mu^2 T^{\kappa}}. \tag{33}$$

Plots of the infinite domain solution for the fractional cable equation in Model I are shown in Fig 1 for different values of γ and κ. The solution is smooth at the origin, similar to the standard diffusion equation, but the rate of decay is affected by the scaling exponents. The decay is faster for short times but slower over long times when diffusion is anomalous.

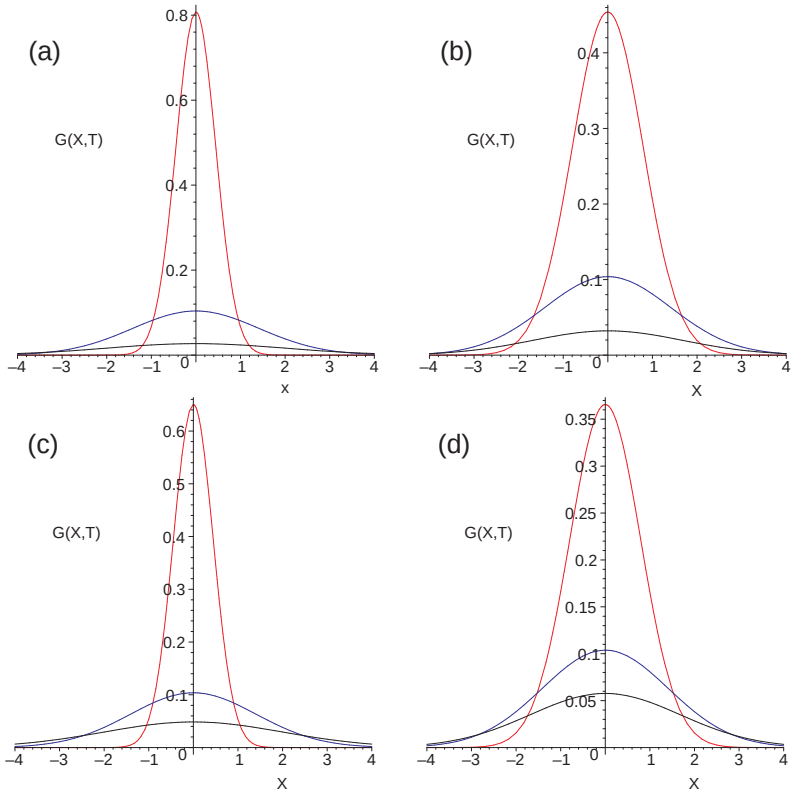

Fig. 1 Plot of the Green's solution for the fractional cable equation, (24) at times $T = 0.1$ (red), $T = 1.0$ (blue), and $T = 2.0$ (black) for: (a) $\gamma = 1.0, \kappa = 1.0$, (b) $\gamma = 0.5, \kappa = 1.0$ (c) $\gamma = 1.0, \kappa = 0.5$ (d) $\gamma = 0.5, \kappa = 0.5$ The parameter $\mu = 1$ in each case.

3.2 Infinite Domain – Model II

In this section we derive the Green's solution for (25) in an infinite cable with no external current and with initial condition $V(X,0) = \delta(X)$. The Green's solution for linear partial differential equations can generally be found using Fourier and Laplace transform methods. The transformed solution is obtained as the solution to an algebraic problem in Fourier-Laplace space and then the Green's solution in the original variables is obtained by carrying

out the inverse transforms. We have followed this approach in the following for the linear fractional cable equation, using the known Laplace transform of the Riemann-Liouville fractional derivative, and using Fox H functions and their properties to facilitate the inverse Laplace transforms. The advantage of using Fox H functions is that derivatives of Fox functions and (inverse) Laplace transforms of Fox functions can be evaluated using index shifting properties (Appendix B).

First we take the Fourier-Laplace transform of (25) using the result that the Laplace transform of the Riemann-Liouville derivative $D_t^\alpha y(t)$ of order α, $0 < \alpha \leq 1$, is given by [26]

$$\mathscr{L}\{D_t^\alpha y(t)\} = s^\alpha \hat{y}(s) - \left(D_t^{\alpha-1} y(t)\right)|_{t=0} \tag{34}$$

to obtain the Green's solution of the fractional cable equation in Fourier-Laplace space, i.e.,

$$\widehat{\widetilde{G}}(q,s) = \frac{1}{s + s^{1-\gamma} q^2 + \mu^2 s^{1-\kappa}}. \tag{35}$$

In this equation q and s are the Fourier and Laplace variables and the tilde and hat denote Fourier and Laplace transformed functions respectively. In the following $\left(D_t^{\alpha-1} y(t)\right)|_{t=0} = 0$ in all cases. In the next step we invert the Fourier transform to obtain

$$\widehat{G}(X,s) = \frac{s^{\frac{\gamma}{2}-1}}{2\sqrt{z}} e^{-\rho\sqrt{z}} \tag{36}$$

where

$$\rho = |X| s^{\frac{\gamma}{2}} \tag{37}$$

and

$$z = 1 + \mu^2 s^{-\kappa}. \tag{38}$$

In order to evaluate the inverse Laplace transform we first expand the Laplace transform as a series expansion in Fox H functions and then we invert this expansion term by term. First we consider the function

$$h(z) = \frac{1}{\sqrt{z}} e^{-\rho\sqrt{z}} \tag{39}$$

which can be written in terms of Fox functions as follows [46]

$$h(z) = \rho H_{0,1}^{1,0}\left[\rho z^{\frac{1}{2}} \,\middle|\, \begin{matrix} - \\ (-1,1) \end{matrix}\right]. \tag{40}$$

The Taylor series expansion for $h(z)$ about $z = 1$ can readily be found using index shifting properties of the Fox functions. The kth derivative of $h(z)$, which follows from the identity (163), is given by;

$$h^{(k)}(z) = \rho z^{-k} H_{1,2}^{1,1}\left[\rho z^{\frac{1}{2}} \,\middle|\, \begin{matrix} (0,\frac{1}{2}) \\ (-1,1)\ (k,\frac{1}{2}) \end{matrix}\right] \tag{41}$$

This can readily be evaluated at $z = 1$ to yield

$$h^{(k)}(1) = \rho H_{1,2}^{1,1}\left[\rho \,\middle|\, \begin{matrix} (0,\frac{1}{2}) \\ (-1,1)\ (k,\frac{1}{2}) \end{matrix}\right] = \frac{2(-1)^k}{\sqrt{4\pi}} H_{0,2}^{2,0}\left[\frac{\rho^2}{4} \,\middle|\, \begin{matrix} - \\ (0,1)\ (k+\frac{1}{2},1) \end{matrix}\right] \tag{42}$$

where the second expression is obtained using: (165) with $c = 2$; (166) with $\alpha = 1$ and $r = k$; (167) with $\sigma = 1/2$; and the Legendre duplication formula for the Gamma function,

$2\sqrt{\pi}\Gamma(2r) = 2^{2r}\Gamma(r)\Gamma(r+\frac{1}{2})$. The Taylor series expansion for $h(z)$ about $z=1$ is thus given by

$$h(z) = \frac{2}{\sqrt{4\pi}} \sum_{k=0}^{\infty} (-1)^k \frac{(z-1)^k}{k!} H_{0,2}^{2,0}\left[\frac{\rho^2}{4} \middle| \begin{matrix} - \\ (0,1)\ \left(\frac{1}{2}+k,1\right) \end{matrix} \right], \tag{43}$$

and then using (36)-(39) and (43) we obtain the series expansion for the Laplace transform

$$\widehat{G}(X,s) = \frac{1}{\sqrt{4\pi}} \sum_{k=0}^{\infty} \frac{\left(-\mu^2\right)^k}{n!} s^{-k\kappa-1+\frac{\gamma}{2}} H_{0,2}^{2,0}\left[\frac{X^2 s^\gamma}{4} \middle| \begin{matrix} - \\ (0,1)\ \left(\frac{1}{2}+k,1\right) \end{matrix} \right]. \tag{44}$$

In order to facilitate the inverse Laplace transform we first use the reduction formula, (168) with $d = 1-\frac{\gamma}{2}+\kappa k$ and $\Delta = \gamma$, to write

$$\widehat{G}(X,s) = \frac{1}{\sqrt{4\pi}} \sum_{n=0}^{\infty} \frac{\left(-\mu^2\right)^k}{k!} s^{-k\kappa+\frac{\gamma}{2}-1} H_{1,3}^{3,0}\left[\frac{X^2 s^\gamma}{4} \middle| \begin{matrix} \left(1-\frac{\gamma}{2}+\kappa k,\gamma\right) \\ \left(1-\frac{\gamma}{2}+\kappa k,\gamma\right)\ (0,1)\ \left(\frac{1}{2}+k,1\right) \end{matrix} \right]. \tag{45}$$

The inverse Laplace transform can then be evaluated term by term using (169) with $\omega = k\kappa - \frac{\gamma}{2}$, $\sigma = \gamma$, and $z = x^2/4$. We finally obtain the solution of the fractional cable equation in the infinite domain

$$G(X,T) = \frac{1}{\sqrt{4\pi T^\gamma}} \sum_{k=0}^{\infty} \frac{\left(-\mu^2 T^\kappa\right)^k}{k!} H_{1,2}^{2,0}\left[\frac{X^2}{4T^\gamma} \middle| \begin{matrix} \left(1-\frac{\gamma}{2}+\kappa k,\gamma\right) \\ (0,1)\ \left(\frac{1}{2}+k,1\right) \end{matrix} \right]. \tag{46}$$

In the limit of large X and large T, asymptotic expressions for the Fox functions [4] can be used to find the asymptotic behaviour of the Green's function in (46);

$$G(X,T) \sim \frac{1}{\sqrt{4\pi T^\gamma}} \frac{1}{\sqrt{2-\gamma}} \left(\frac{2}{\gamma}\right)^{\frac{1-\gamma}{2-\gamma}} \left(\frac{|X|}{T^{\frac{\gamma}{2}}}\right)^{-\frac{1-\gamma}{2-\gamma}} \exp\left(-\frac{(2-\gamma)}{2} \left(\frac{\gamma}{2}\right)^{\frac{\gamma}{2-\gamma}} \left(\frac{|X|}{T^{\frac{\gamma}{2}}}\right)^{\frac{2}{2-\gamma}} \right) \exp\left(-\mu^2 \frac{T^\kappa}{\gamma} \left(\frac{\gamma|X|}{2T^{\frac{\gamma}{2}}}\right)^{\frac{2(1-\kappa)}{2-\gamma}} \right). \tag{47}$$

The Green's solution for the fractional cable equation (25) in an infinite domain is plotted in Fig. 2 (with $\mu = 1$) for times $T = 0.1$, 1.0, and 10.0 and with different values of γ and κ. Note in the case of standard diffusion $\gamma = \kappa = 1$ the Green's solution is essentially zero at $T = 10.0$ and cannot be distinguished from the axis in Fig. 2(a). It can also be seen that the Green's solution decays to zero for large $|X|$ and is an even function of X. In each case, the solution decays to zero for large T. It is interesting to note that in Fig. 2(a) and Fig.2(c), where the diffusion along the axial direction of the cable is standard ($\gamma = 1$), the derivative of the solution is continuous at $X = 0$. This contrasts with the anomalous diffusion case ($\gamma = 1/2$) where the derivative is discontinuous at $X = 0$ (see Fig. 2(b) and Fig. 2(d)). The fractional derivative effectively "remembers" the discontinuity of the second derivative in the initial condition. An interesting finding, in the case $\gamma = 1/2$ and $\kappa = 1$ (Fig. 2(b)) is that the solution becomes negative near $X = 0$. The negative solution is not unphysical ($G(X,T)$ is not a probability density) and it does not contradict the asymptotic large X and T behaviour, (47), where the solution is predicted to remain positive for sufficiently large X.

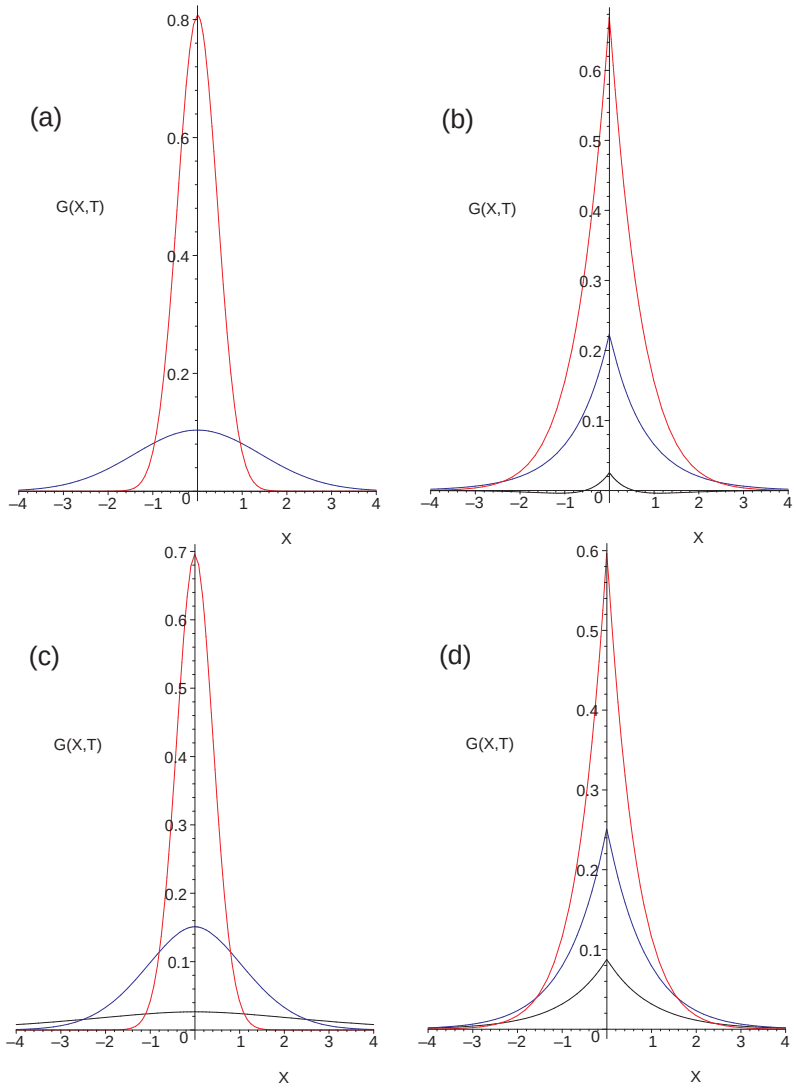

Fig. 2 The Green's solution of the fractional cable equation (25) in an infinite domain at times $T = 0.1$ (red), $T = 1.0$ (blue), and $T = 10.0$ (black) for: (a) $\gamma = 1.0, \kappa = 1.0$, (b) $\gamma = 0.5, \kappa = 1.0$ (c) $\gamma = 1.0, \kappa = 0.5$ (d) $\gamma = 0.5, \kappa = 0.5$ The parameter $\mu = 1$ in each case.

A further comparison of the Green's solutions at corresponding times T but different values of γ and κ are shown in Fig. 3. At short times, as shown in Fig. 3(a), the peak height decreases faster when the diffusion is anomalous (either along the neuron $\gamma < 1$ or across the membrane $\kappa < 1$). This trend reverses on longer times, Figs. 3(b), 3(c). The negative potential in the case $\gamma = 0.5, \kappa = 1.0$ can clearly be seen on this magnified scale in Fig. 3(d)

The rate of spreading of the Green's solution can also be seen by investigating the second moment $\langle X^2(t) \rangle$ where the angular bracket denotes the 'average' with respect to the Green's

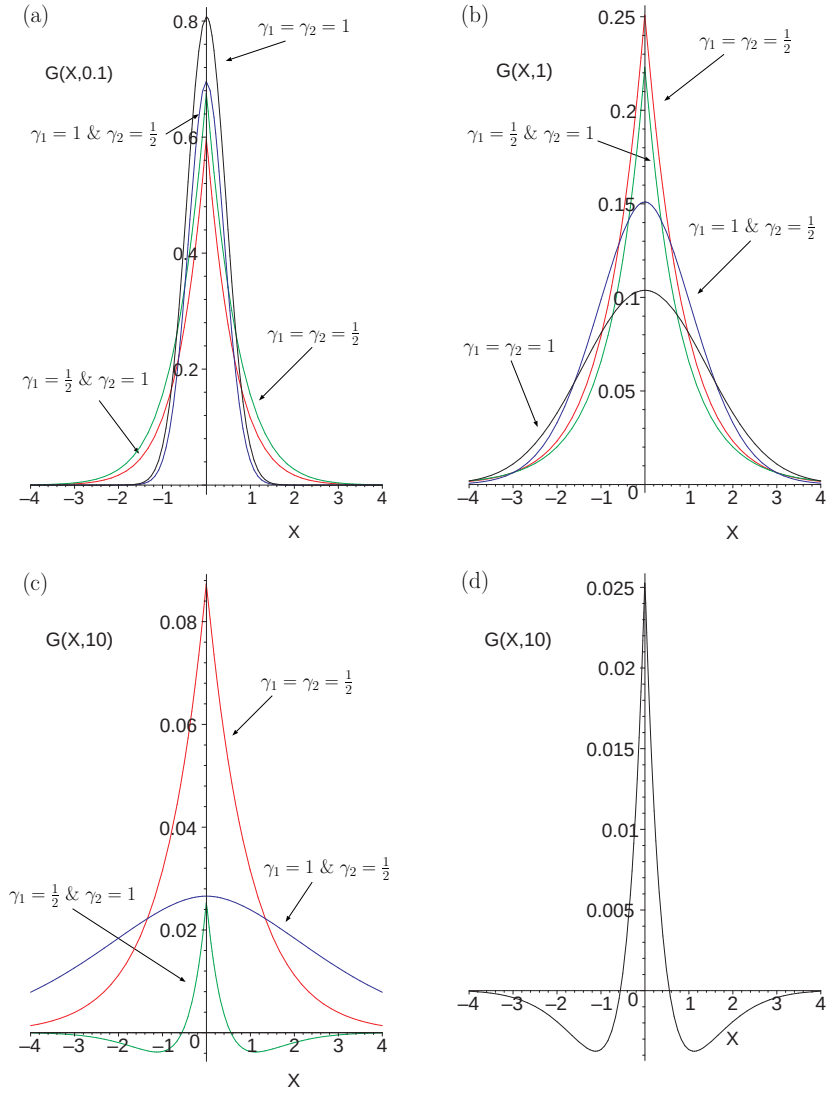

Fig. 3 Green's solution of the fractional cable equation (25) in an infinite cable at (a) $T=0.1$, (b) $T=1$, and (c) $T=10$ for different values of $\gamma=\gamma_1$ and $\kappa=\gamma_2$ as indicated. The Green's solution at $T=10$ with $\gamma=\gamma_1=0.5$ and $\kappa=\gamma_2=1.0$ is shown in (d).

solution, i.e.,

$$\langle X^2(T)\rangle = \int_{-\infty}^{\infty} G(X,T)X^2\,dX.$$

Note that the second moment is not necessarily positive since $G(X,T)$ is not strictly positive. The second moment can be evaluated using the Fourier-Laplace representation

$$\langle X^2(T)\rangle = \mathscr{L}^{-1}\left(\lim_{q\to 0} -\frac{d^2}{dq^2}\widehat{\widetilde{G}}(q,s)\right).$$

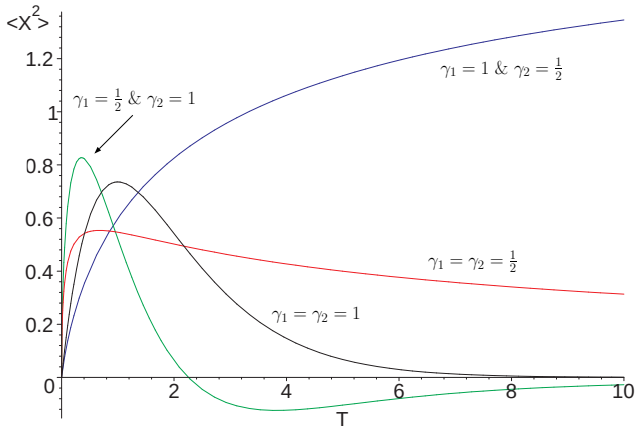

Fig. 4 A comparison of the second moment for different values of $\gamma = \gamma_1$ and $\kappa = \gamma_2$ as indicated.

Using the expression for $\widehat{\widetilde{G}}(q,s)$ in (35) we have

$$\left\langle X^2(T)\right\rangle = \mathscr{L}^{-1}\left(\frac{2s^{\kappa-(1+\gamma-\kappa)}}{(s^\kappa+\mu^2)^2}\right)$$

and then evaluating the inverse Laplace transform in terms of the generalized Mittag-Leffler function [26] we have

$$\left\langle X^2(T)\right\rangle = 2T^\gamma E^{(1)}_{\kappa,1+\gamma-\kappa}\left(-\mu^2 T^\kappa\right). \tag{48}$$

A plot of the second moment as a function of time T is shown in Fig. 4 for different values of γ and κ. In the case where $\gamma = 0.5$ and $\kappa = 1.0$ the second moment becomes negative, which is a result of the Green's solution becoming negative. The physical interpretation of this (see e.g., (14)) is that the current switches directions for these parameter values.

The possible negativity of $\langle X^2\rangle$ makes it difficult to relate the behaviour of $\langle X^2\rangle/T$ to an apparent diffusion coefficient. However it is clear from Fig. 4 that $\langle X^2\rangle/T$ exhibits a time dependent crossover in scaling behaviour (increasing or constant at short times but decreasing at long times) and this is broadly similar to crossover scaling behaviour in the apparent diffusion coefficient for ageing continuous time random walks (constant at short times and decreasing at long times [2]).

4 Input Current Response

The infinite domain Green's solutions, (33) and (46), corresponding to Model I, (24), and Model II, (25), respectively were obtained for initial condition $V(X,0) = \delta(X)$ and no external current. It follows from the linearity of the fractional cable equations that general solutions for non-zero external current densities and general initial condition $V(X,0) = V_0(X)$ can be obtained from the Green's solutions. Explicitly, the general solutions for (24) and (25) can be expressed as,

$$\begin{aligned} V_I(X,T) = &\int_{-\infty}^{\infty} V_I(X',0)G_I(X-X',T')\,dX' \\ &+\mu^2\kappa\int_{-\infty}^{\infty}\int_0^T G_I(X-X',T-T')T'^{\kappa-1}\left[i_e r_m\right](X',T')\,dT'\,dX', \end{aligned} \tag{49}$$

and

$$V_{II}(X,T) = \int_{-\infty}^{\infty} V_{II}(X',0)G_{II}(X-X',T')\,dX' + \mu^2 \int_{-\infty}^{\infty}\int_0^T G_{II}(X-X',T-T')\frac{\partial^{1-\kappa}}{\partial T'^{1-\kappa}}\left[i_e r_m\right](X',T')\,dT'\,dX', \quad (50)$$

respectively, where the subscripts I and II are used to label the different models. The general solution for Model I can also be obtained from

$$V_I(X,T) = e^{-\mu^2 T^\kappa} W(X,S) \quad (51)$$

where

$$W(X,S) = \int_{-\infty}^{\infty} W(X',0)G^*(X-X',S)\,dX' + \mu^2\theta \int_{-\infty}^{\infty}\int_0^S G^*(X-X',S-S')S'^{\theta-1}e^{\mu^2 S'^\theta}\left[i_e r_m\right](X',S'^{\frac{1}{\gamma}})\,dT'\,dS', \quad (52)$$

$G^*(X,S)$ is the Green's solution, (32), for the standard diffusion equation, and $\theta = \kappa/\gamma$.

In theoretical studies of the standard linear cable equation, common inputs that have been considered include [49]; a spike function $\delta(X-X_0)\delta(T)$, a step function $\delta(X-X_0)\left(1-H(T-\tau)\right)$, and an alpha function $\delta(X-X_0)Te^{-\alpha T}$. Here we consider similar inputs for the fractional linear cable equations, (24) and (25), by first defining an input function $f(T)$ with one of the functional forms (spike, step or alpha function) and then defining associated external current densities i_e in one of two ways;

$$f(X,T) = i_e r_m \quad (53)$$

or

$$f(X,T) = \mathscr{D}^*(\kappa,T)\left(i_e r_m\right) \quad (54)$$

where

$$\mathscr{D}^*(\kappa,T) = \kappa T^{\kappa-1} \qquad \text{Model I}$$

and

$$\mathscr{D}^*(\kappa,T) = \frac{\partial^{1-\kappa}}{\partial T^{1-\kappa}} \qquad \text{Model II}$$

In the following we describe results for an instantanenous input with external current defined by (54) and for an alpha function input with external current defined by (53).

4.1 Instantaneous Input

In the case of an input instantaneous input

$$f(X,T) = \delta(X-X_0)\delta(T) \quad (55)$$

with zero initial condition, $V(X,0) = 0$, and external current defined by (54) the solutions reduce to $V(X,T) = G_I(X-X_0,T)$ (Model I) and $V(X,T) = G_{II}(X-X_0,T)$ (Model II). These solutions are equivalent to solutions of the linear fractional cable equations with zero external current, $i_e = 0$, and with initial condition $V(X,0) = \delta(X-X_0)$. In a recent letter [16] we considered these solutions for $\gamma = \kappa$ with $X_0 = 1$ and found that the peak potential

arrives at the soma $X = 0$ earlier with decreasing γ and the potential is maintained at elevated levels for longer times with decreasing γ. In Fig. 5 we show plots of $V(X,0)$ for the same initial conditions but a wider range of γ and κ including cases with $\gamma \neq \kappa$. If $\kappa = 1$ then the peak arrives at the soma earlier with decreasing γ but if $\gamma = 1$ the peak arrives at the soma later with decreasing κ. These features are broadly similar in both models.

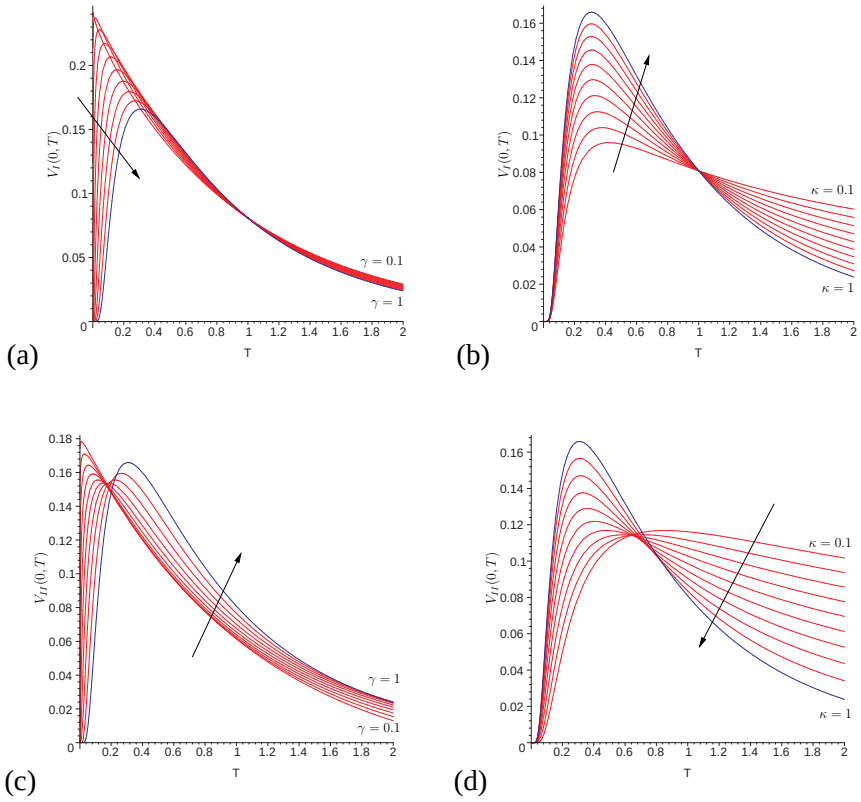

Fig. 5 Plots of $V(0,T)$ in response to an instantaneous unit input at $X = 1$. (a) Model I $\kappa = 1.0$, (b) Model I $\gamma = 1.0$ (c) Model II $\kappa = 1.0$ (d) Model II $\gamma = 1.0$ The parameter $\mu = 1$ in each case.

4.2 Alpha Function Input

We now consider alpha function inputs

$$f(T) = \delta(X - X_0)\beta T e^{-\alpha T} \tag{56}$$

with zero initial condition, $V(X,0) = 0$, and with i_e defined by (53). In this case the input is modulated by the fractional temporal operators in (49) and (50).

4.2.1 Alpha Function Input – Model I

We first substitute the alpha function input, (56), with external current density, (53) into (52) with $W(X',0)=0$ to obtain

$$W(X,S)=\beta\theta\mu^2\int_0^S G^*(X-X_0,S-S')\,S^{\frac{1}{\gamma}+\theta-1}e^{\mu^2S'^{\theta}}e^{-\alpha S'^{\frac{1}{\gamma}}}\,dS'. \tag{57}$$

To evaluate the integral, we expand the exponential term $e^{\mu^2S'^{\theta}}$ as a Taylor series in S' and take a Fourier transform of $G^*(X-X_0,S-S')$ with respect to X. This yields

$$\tilde{W}(q,S)=e^{-iqX_0}\beta\theta\mu^2\sum_{k=0}^{\infty}\frac{\mu^{2k}}{k!}\int_0^S e^{-q^2(S-S')}\,z^{\frac{1}{\gamma}+\theta(k+1)-1}e^{-\alpha S'^{\frac{1}{\gamma}}}\,dS'. \tag{58}$$

The remaining exponential terms can be represented as Fox functions

$$e^{-\alpha S'^{\frac{1}{\gamma}}}=H_{0,1}^{1,0}\left[\alpha S'^{\frac{1}{\gamma}}\,\middle|\,\begin{matrix}-\\(0,1)\end{matrix}\right], \tag{59}$$

$$e^{-q^2(S-S')}=H_{0,1}^{1,0}\left[q^2\left(S-S'\right)\,\middle|\,\begin{matrix}-\\(0,1)\end{matrix}\right], \tag{60}$$

and the resulting integral can be simplified using the Fox function convolution identity (171). This results in

$$\tilde{W}(q,S)=e^{-iqX_0}\beta\theta\mu^2S^{\frac{1}{\gamma}+\theta}\sum_{k=0}^{\infty}\frac{\left(\mu^2S^{\theta}\right)^k}{k!}\sum_{r=0}^{\infty}\frac{\left(-\alpha s^{\frac{1}{\gamma}}\right)^r}{r!}\Gamma\left(\frac{1+r}{\gamma}+\theta\left(1+k\right)\right)$$
$$H_{1,2}^{1,1}\left[q^2S\,\middle|\,\begin{matrix}(0,1)\\(0,1)\ \left(-\frac{1+r}{\gamma}-\theta\left(1+k\right),1\right)\end{matrix}\right]. \tag{61}$$

After taking the inverse Fourier Transform we now arrive at

$$W(X,S)=\frac{\beta\theta\mu^2S^{\frac{1}{\gamma}+\theta}}{\sqrt{4\pi S}}\sum_{k=0}^{\infty}\frac{\left(\mu^2S^{\theta}\right)^k}{k!}\sum_{r=0}^{\infty}\frac{\left(-\alpha S^{\frac{1}{\gamma}}\right)^r}{r!}\Gamma\left(\frac{1+r}{\gamma}+\theta\left(1+k\right)\right)$$
$$H_{1,2}^{1,1}\left[\frac{(X-X_0)^2}{4u}\,\middle|\,\begin{matrix}\left(\frac{1}{2}+\frac{r+1}{\gamma}+\theta\left(k+1\right),1\right)\\(0,1)\qquad\left(\frac{1}{2},1\right)\end{matrix}\right] \tag{62}$$

and the final solution that follows from (51) is

$$V(X,T)=\frac{\kappa\mu^2\beta T^{1+\kappa}e^{-\mu^2T^{\kappa}}}{\gamma\sqrt{4\pi T^{\gamma}}}\sum_{k=0}^{\infty}\frac{\left(\mu^2T^{\kappa}\right)^k}{k!}\sum_{r=0}^{\infty}\frac{(-\alpha T)^r}{r!}\Gamma\left(\frac{1+r+\kappa(k+1)}{\gamma}\right)$$
$$H_{1,2}^{2,0}\left[\frac{(X-X_0)^2}{4T^{\gamma}}\,\middle|\,\begin{matrix}\left(\frac{1}{2}+\frac{1+r+\kappa(k+1)}{\gamma},1\right)\\(0,1)\qquad\left(\frac{1}{2},1\right)\end{matrix}\right]. \tag{63}$$

In the case of standard diffusion and standard current ($\gamma = \kappa = 1$) this solution reduces to

$$V(X,T) = \frac{\mu^2 \beta e^{-\alpha T}}{\sqrt{4\pi}} \left[T I_1 \left(X - X_0, T \right) - I_2 \left(X - X_0, T \right) \right] \tag{64}$$

where for $\rho > 0$

$$I_1(X,T) = \frac{\sqrt{\pi}}{2\rho} \left[e^{-\rho |X|} \text{erfc} \left(\sqrt{\frac{X^2}{4T}} - \rho \sqrt{T} \right) - e^{\rho |X|} \text{erfc} \left(\sqrt{\frac{X^2}{4T}} + \rho \sqrt{T} \right) \right], \tag{65}$$

$$I_2(X,T) = -\frac{\sqrt{T}}{\rho^2} e^{-\frac{X^2}{4T} - \rho^2 T} + \frac{\sqrt{\pi}}{4\rho^3} \left[\left(\rho |X| + 1 \right) e^{-\rho |X|} \text{erfc} \left(\sqrt{\frac{X^2}{4T}} - \rho \sqrt{T} \right) \right.$$
$$\left. + \left(\rho |X| - 1 \right) e^{\rho |X|} \text{erfc} \left(\sqrt{\frac{X^2}{4T}} + \rho \sqrt{T} \right) \right], \tag{66}$$

and for $\rho = 0$

$$I_1(X,T) = 2\sqrt{T} e^{-\frac{X^2}{4T}} - |X| \sqrt{\pi} \text{erfc} \left(\sqrt{\frac{X^2}{4T}} \right), \tag{67}$$

$$I_2(X,T) = \frac{2}{3} T^{3/2} e^{-\frac{X^2}{4T}} - \frac{X^2}{3} \sqrt{T} e^{-\frac{X^2}{4T}} + \frac{|X|^3 \sqrt{\pi}}{6} \text{erfc} \left(\sqrt{\frac{X^2}{4T}} \right), \tag{68}$$

where $\rho = \sqrt{\mu^2 - \alpha}$.

4.2.2 Alpha Function Input – Model II

We now consider the potential, (49), in response to the alpha function input, (56), with external current density defined by, (53), and with initial potential $V(X',0) = 0$. The resulting potential is given by

$$V(X,T) = \mu^2 \beta \int_0^T G(X - X_0, T - T') \frac{\partial^{1-\kappa}}{\partial T'^{1-\kappa}} \left(T' e^{-\alpha T'} \right) dT' \tag{69}$$

where $G(X,T)$ is the Greens solution in (46). The fractional integral can readily be evaluated to yield

$$V(X,T) = \mu^2 \beta \int_0^T G(X - X_0, T') \left(T - T' \right)^{\kappa} E_{1,\kappa}^{(1)} \left(-\alpha (T - T') \right) dT'. \tag{70}$$

where

$$E_{1,\kappa}^{(1)} \left(-\alpha (T - T') \right) = \sum_{j=0}^{\infty} \frac{j+1}{\Gamma \left(j + 1 + \kappa \right)} \left(-\alpha (T - T') \right)^j \tag{71}$$

is the Mittag-Leffler function [27]. The potential can thus be written as

$$V(X,T) = \mu^2\beta \sum_{j=0}^{\infty} \frac{(j+1)(-\alpha)^j}{\Gamma(j+1+\kappa)} \int_0^T \frac{G(X-X_0,T')}{(T-T')^{1-(\kappa+j+1)}}\, dT' \tag{72}$$

$$= \mu^2\beta \sum_{j=0}^{\infty} (j+1)(-\alpha)^j \frac{\partial^{-(\kappa+1+j)}}{\partial T^{-(\kappa+1+j)}} G(X-X_0,T). \tag{73}$$

The fractional integral of the Green's solution can be evaluated and simplified using the identities (166) and (168) to yield

$$V(X,T) = \frac{\mu^2\beta T^{1+\kappa}}{\sqrt{4\pi T^{\gamma}}} \sum_{k=0}^{\infty} \frac{\left(-\mu^2 T^{\kappa}\right)^k}{k!} \sum_{j=0}^{\infty} (j+1)(-\alpha T)^j$$
$$H_{1,2}^{2,0}\left[\frac{(X-X_0)^2}{4T^{\gamma}} \,\middle|\, \begin{matrix} \left(2-\frac{\gamma}{2}+\kappa(k+1)+j,\gamma\right) & \\ (0,1) & \left(\frac{1}{2}+k,1\right) \end{matrix} \right]. \tag{74}$$

In the case of standard diffusion and standard current ($\gamma = \kappa = 1$) the solutions represented in (64)–(68) are recovered.

Figure 6 shows the temporal behaviour of the potential at the origin for Model I (left) and Model II (right) in response to an alpha function input at $X_0 = 1$ with equal exponents $\gamma = \kappa$. Other parameters, α, β, μ have been set to unity in these plots. In each of the models the peak height increases as the exponent γ increases. The arrival of the peak at the soma is earlier with increasing γ in Model I but earlier with decreasing γ in Model II.

5 Semi-Infinite Domain Solutions

In this section we consider solutions of the fractional cable equations on semi-infinite domains $X \geq 0$ with initial condition $V(X,0) = \delta(X-Y)$ and with prescribed boundary conditions at $X = 0$. This solution represents the response to an instantaneous unit input at $X = Y$ with Green's functions corresponding to $Y = 0$. Solutions for other input functions could be obtained using these Green's functions as described for infinite cables in the preceding section. The main purpose of introducing the semi-infinite cable here is to describe solution methods for more realistic boundary conditions. Three different boundary conditions are considered:

(i) Voltage clamped

$$V(0,T) = V_0 \tag{75}$$

(ii) Constant fractional axial current

$$-D^{\star}(\gamma)\mathscr{D}^{\star}(\gamma,T)\frac{\partial V}{\partial X} = V_0' \tag{76}$$

(iii) Constant standard axial current

$$-\frac{1}{D^{\star}(\gamma)}\frac{\partial V}{\partial X} = V_0' \tag{77}$$

where V_0' is a constant and

$$D^{\star}(\gamma) = \sqrt{\tau_m^{\gamma-1} D(\gamma)}. \tag{78}$$

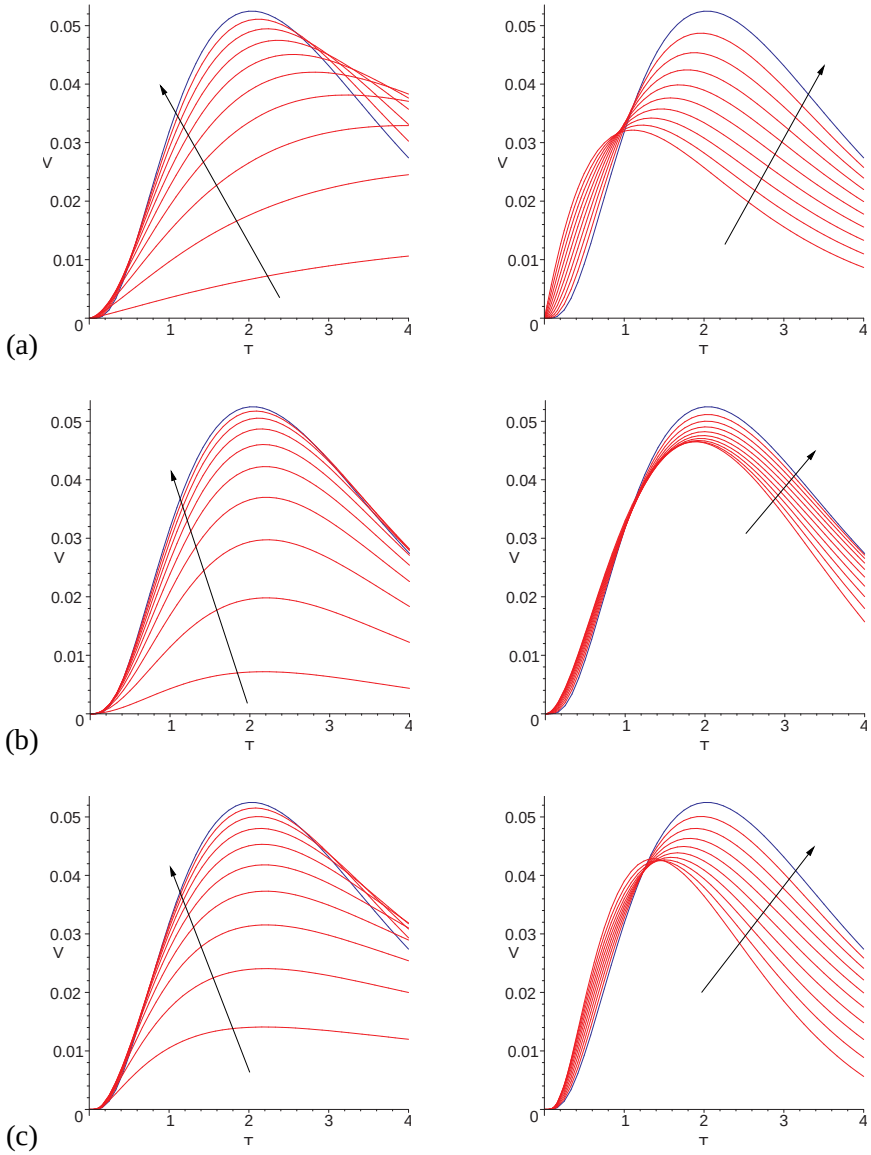

Fig. 6 Voltage at the soma $X = 0$ in response to alpha function input at $X_0 = 1$ for: (a) $\gamma = \kappa = 0.1, 0.2, 0.3, \ldots 1.0$. (b) $\kappa = 1.0$. (c) $\gamma = 1.0$. The results for Model I are shown at left and results for Model II are shown at right. The arrows indicate plots with increasing γ or increasing κ.

To simplify the algebra in the following we consider solutions with $D^\star(\gamma) = 1$. Killed end boundary conditions and sealed end boundary conditions can be obtained as special cases with $V_0 = 0$ and $V_0' = 0$ respectively.

5.1 Semi-Infinite Domain – Model I

As in section 3.1 we consider the change of variables from $V(X,T)$ to $W(X,S)$ defined by (29), (30) and we proceed to find the solution using Laplace transform methods with respect to the variable S. The Laplace transform of the resulting diffusion equation for $W(X,S)$ yields

$$\frac{\partial^2 \widehat{W}}{\partial X^2} - \lambda^2(s)\widehat{W} = -\delta(X-Y) \tag{79}$$

with algebraic solution

$$\widehat{W} = A(s)e^{\lambda(s)X} + B(s)e^{-\lambda(s)X} - \frac{1}{\lambda(s)} \begin{cases} 0, & X < Y \\ \sinh[\lambda(s)(X-Y)], & X \geq Y \end{cases} \tag{80}$$

where A and B are arbitrary constants and $\lambda(s) = \sqrt{s}$. To ensure the solution is bounded as $X \to \infty$ we require

$$A(s) = \frac{1}{\lambda(s)} \frac{e^{-\lambda(s)Y}}{2}. \tag{81}$$

(80) can then be written as

$$\widehat{W}(X,s) = \frac{1}{2\lambda(s)} e^{-\lambda(s)|X-Y|} + B(s)e^{-\lambda(s)X}. \tag{82}$$

The value of $B(s)$ can now be determined from the boundary condition at $X = 0$ using one of the following equations,

$$B(s) = \widehat{W}(0,s) - \frac{1}{2\lambda(s)} e^{-\lambda(s)|Y|},$$

$$B(s) = -\frac{1}{\lambda(s)} \frac{\partial \widehat{W}}{\partial X}\bigg|_{X=0} + \frac{1}{2\lambda(s)} e^{-\lambda(s)|Y|}.$$

Here we consider the three boundary conditions for $V(X,T)$ described in equations (75) – (77) which yield the corresponding boundary conditions for $W(X,S)$
(i) Voltage clamped

$$W(0,S) = V_o e^{\mu^2 S^\theta} = W_1(S) \tag{83}$$

(ii) Constant fractional axial current

$$\frac{\partial W}{\partial X}(0,S) = -\frac{V_o'}{\gamma S^{1-1/\gamma}} e^{\mu^2 S^\theta} = -W_2(S) \tag{84}$$

(iii) Constant standard axial current

$$\frac{\partial W}{\partial X}(0,S) = -\frac{V_o'}{e^{\mu^2 S^\theta}} = -W_3(S) \tag{85}$$

where $\theta = \frac{\kappa}{\gamma}$.

Using the Laplace transforms of the boundary conditions, (83)–(85) as above we obtain:
(i)

$$\widehat{W}(X,s) = \widehat{W}_1(s)e^{-\lambda(s)X} + \frac{1}{2\lambda(s)} e^{-\lambda(s)|X-Y|} - \frac{1}{2\lambda(s)} e^{-\lambda(s)(X+Y)}, \tag{86}$$

(ii)

$$\widehat{W}(X,s) = \frac{\widehat{W}_2(s)}{\lambda(s)} e^{-\lambda(s)X} + \frac{1}{2\lambda(s)} e^{-\lambda(s)|X-Y|} + \frac{1}{2\lambda(s)} e^{-\lambda(s)(X+Y)}, \tag{87}$$

(iii)

$$\widehat{W}(X,s) = \frac{\widehat{W}_3(s)}{\lambda(s)} e^{-\lambda(s)X} + \frac{1}{2\lambda(s)} e^{-\lambda(s)|X-Y|} + \frac{1}{2\lambda(s)} e^{-\lambda(s)(X+Y)}. \tag{88}$$

Note in each case the last two terms are simply the Laplace transform of the infinite domain solution of the diffusion equation (31) with initial conditions $W(X,0) = \delta(X-Y)$ and $W(X,0) = \delta(X+Y)$ respectively, and so it only remains to find the inverse Laplace transform of the first term. In each case this yields a convolution integral that can be expressed as a series expansion in terms of Fox H functions.

Case (i)

The first term in (86),

$$\widehat{\phi}_1(s) = \widehat{W}_1(s) e^{-\lambda(s)X}, \tag{89}$$

can be inverted using the Laplace convolution formula

$$\mathscr{L}^{-1}\left\{ \widehat{f}(s)\widehat{g}(s) \right\} = \int_0^S f(S-z)g(z)\,dz \tag{90}$$

together with (83) and the result,

$$\mathscr{L}\left\{ \frac{X}{\sqrt{4\pi S^3}} e^{-\frac{X^2}{4S}} \right\}(s) = e^{-\lambda(s)X}.$$

This yields

$$\phi_1(S) = \frac{V_0 X}{\sqrt{4\pi}} \int_0^S z^{-3/2} e^{\mu^2 (S-z)^\theta} e^{-\frac{X^2}{4z}}\, dz. \tag{91}$$

The above convolution integral can be evaluated as a series expansion in terms of H functions. To see this we expand the first exponential on the right hand side of (91) as a Taylor series giving

$$\phi_1(S) = \frac{V_0 X}{\sqrt{4\pi}} \sum_{k=0}^{\infty} \frac{\left(\mu^2\right)^k}{k!} \int_0^S \frac{z^{-3/2} e^{-\frac{X^2}{4z}}}{(S-z)^{1-(1+\theta k)}}\, dz \tag{92}$$

and then we identify the integral as a fractional integral, i.e.,

$$\phi_1(S) = \frac{V_0 X}{\sqrt{4\pi}} \sum_{k=0}^{\infty} \frac{\left(\mu^2\right)^k}{k!} \Gamma(1+\theta k) \frac{\partial^{-1-\theta k}}{\partial S^{-1-\theta k}} \left\{ S^{-3/2} e^{-\frac{X^2}{4S}} \right\}. \tag{93}$$

The fractional integrals can be evaluated in terms of Fox functions [46] to yield

$$\phi_1(S) = \frac{V_0 X}{\sqrt{4\pi S}} \sum_{k=0}^{\infty} \frac{\left(\mu^2 S^\theta\right)^k}{k!} \Gamma(\theta k+1) H_{1,2}^{2,0}\left[\frac{X^2}{4S} \,\middle|\, \begin{matrix} \left(\frac{1}{2}+\theta k, 1\right) \\ \left(-\frac{1}{2}, 1\right)\ (0,1) \end{matrix} \right]. \tag{94}$$

We obtain the final solution of the fractional cable equation, (24), for this case by combining (29), (30), (86), (89) and (94). The result is

$$V(X,T) = \frac{V_o X\, e^{-\mu^2 T^\kappa}}{\sqrt{4\pi T^\gamma}} \sum_{k=0}^{\infty} \frac{\left(\mu^2 T^\kappa\right)^k}{k!} \Gamma\left(\frac{\kappa}{\gamma}k+1\right) H_{1,2}^{2,0}\left[\frac{X^2}{4T^\gamma}\,\middle|\, \begin{matrix}\left(\frac{1}{2}+\frac{\kappa}{\gamma}k,1\right)\\ \left(-\frac{1}{2},1\right)\ (0,1)\end{matrix}\right] + \frac{1}{\sqrt{4\pi T^\gamma}} e^{-\frac{(X-Y)^2}{4T^\gamma}-\mu^2 T^\kappa} - \frac{1}{\sqrt{4\pi T^\gamma}} e^{-\frac{(X+Y)^2}{4T^\gamma}-\mu^2 T^\kappa} \quad (95)$$

which can be re-written, using (167) with $\sigma = 1/2$, as follows

$$V(X,T) = \frac{V_o\, e^{-\mu^2 T^\kappa}}{\sqrt{\pi}} \sum_{k=0}^{\infty} \frac{\left(\mu^2 T^\kappa\right)^k}{k!} \Gamma\left(\frac{\kappa}{\gamma}k+1\right) H_{1,2}^{2,0}\left[\frac{X^2}{4T^\gamma}\,\middle|\, \begin{matrix}\left(1+\frac{\kappa}{\gamma}k,1\right)\\ (0,1)\ \left(\frac{1}{2},1\right)\end{matrix}\right] + \frac{1}{\sqrt{4\pi T^\gamma}} e^{-\frac{(X-Y)^2}{4T^\gamma}-\mu^2 T^\kappa} - \frac{1}{\sqrt{4\pi T^\gamma}} e^{-\frac{(X+Y)^2}{4T^\gamma}-\mu^2 T^\kappa}. \quad (96)$$

In the case of standard diffusion $\gamma = \kappa = 1$ this solution reduces to

$$V(X,T) = \frac{V_o}{2}\left[e^{-\mu X}\mathrm{Erfc}\left(\sqrt{\frac{X^2}{4T}}-\mu\sqrt{T}\right) + e^{\mu X}\mathrm{Erfc}\left(\sqrt{\frac{X^2}{4T}}+\mu\sqrt{T}\right)\right] + \frac{1}{\sqrt{4\pi T}} e^{-\frac{(X-Y)^2}{4T}-\mu^2 T} - \frac{1}{\sqrt{4\pi T}} e^{-\frac{(X+Y)^2}{4T}-\mu^2 T}. \quad (97)$$

In Fig 7 we show plots of the solution, (95), for various values of γ and κ with $V_0 = 1$ and $V(X,0) = \delta(X-1)$ (i.e., $Y = 1$). Note that when the axial diffusion is standard, $\gamma = 1$, the peak takes longer to decay than when the axial diffusion is anomalous, $\gamma = 0.5$. In these semi-infinite cable solutions the derivative is continuous in all cases.

Case (ii)

The first term in (87),

$$\widehat{\phi}_2(s) = \widehat{W}_2(s) e^{-\lambda(s)X}, \quad (98)$$

can be inverted using the Laplace convolution formula, (90), together with (84) and the result,

$$\mathscr{L}\left\{\frac{1}{\sqrt{4\pi S}} e^{-\frac{X^2}{4S}}\right\}(s) = \frac{1}{2\lambda(s)} e^{-\lambda(s)X}.$$

This yields

$$\phi_2(S) = \frac{2V_o'}{\gamma\sqrt{4\pi}} \int_0^S (S-z)^{\frac{1}{\gamma}-1} e^{\mu^2(S-z)^\theta} z^{-1/2} e^{-\frac{X^2}{4z}}\, dz. \quad (99)$$

Proceeding as above we can write this as a series expansion in terms of H functions,

$$\phi_2(S) = \frac{2V_o' S^{1/\gamma}}{\gamma\sqrt{4\pi S}} \sum_{k=0}^{\infty} \frac{\left(\mu^2 S^\theta\right)^k}{k!} \Gamma\left(\theta k+\frac{1}{\gamma}\right) H_{1,2}^{2,0}\left[\frac{X^2}{4u}\,\middle|\, \begin{matrix}\left(\frac{1}{2}+\frac{1}{\gamma}+\theta k,1\right)\\ (0,1)\quad \left(\frac{1}{2},1\right)\end{matrix}\right]. \quad (100)$$

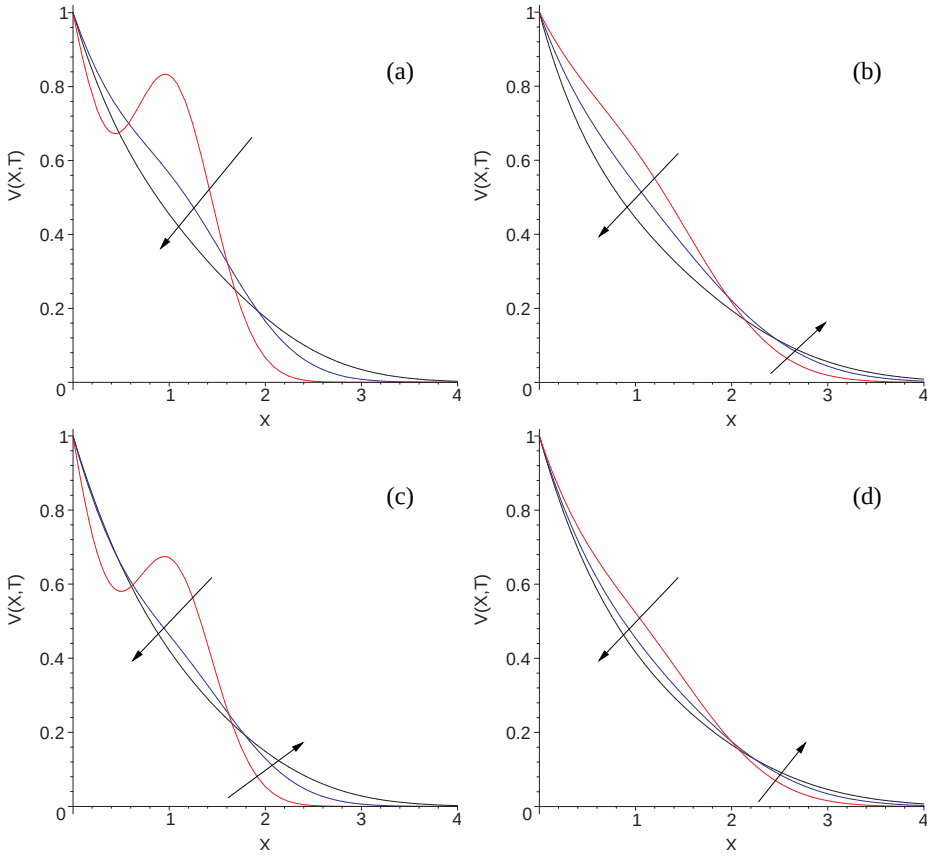

Fig. 7 Plot of (95) with $V(X,0)=\delta(X-1)$ and the fixed boundary condition $V_0=1$ at times $T=0.1$, 0.25, and 0.5 for (a) $\gamma=1.0$, $\kappa=1.0$, (b) $\gamma=0.5$, $\kappa=1.0$, (c) $\gamma=1.0$, $\kappa=0.5$, and (d) $\gamma=0.5$, $\kappa=0.5$. Time increases in the direction of the arrow.

The solution of the fractional cable equation, (24), that now follows from (29), (30), (87), (98), (100) in this case is given by

$$V(X,T)=\frac{2V_o' T\, e^{-\mu^2 T^\kappa}}{\gamma\sqrt{4\pi T^\gamma}}\sum_{k=0}^{\infty}\frac{\left(\mu^2 T^\kappa\right)^k}{k!}\Gamma\left(\frac{\kappa}{\gamma}k+\frac{1}{\gamma}\right)H_{1,2}^{2,0}\left[\frac{x^2}{4T^\gamma}\,\middle|\,\begin{matrix}\left(\frac{1}{2}+\frac{1}{\gamma}+\frac{\kappa}{\gamma}k,1\right)\\(0,1)\end{matrix}\quad\begin{matrix}\\\left(\frac{1}{2},1\right)\end{matrix}\right]$$
$$+\frac{1}{\sqrt{4\pi T^\gamma}}e^{-\frac{(X-Y)^2}{4T^\gamma}-\mu^2 T^\kappa}+\frac{1}{\sqrt{4\pi T^\gamma}}e^{-\frac{(X+Y)^2}{4T^\gamma}-\mu^2 T^\kappa}. \quad (101)$$

Plots of the solution, (101), for various values of γ and κ and with $V_0'=1$ and $Y=1$ are shown in Fig. 8. Note again that the peak at $X=1$ decays more slowly in time T when the axial diffusion is standard, $\gamma=1$, then when it is anomalous, $\gamma=0.5$.

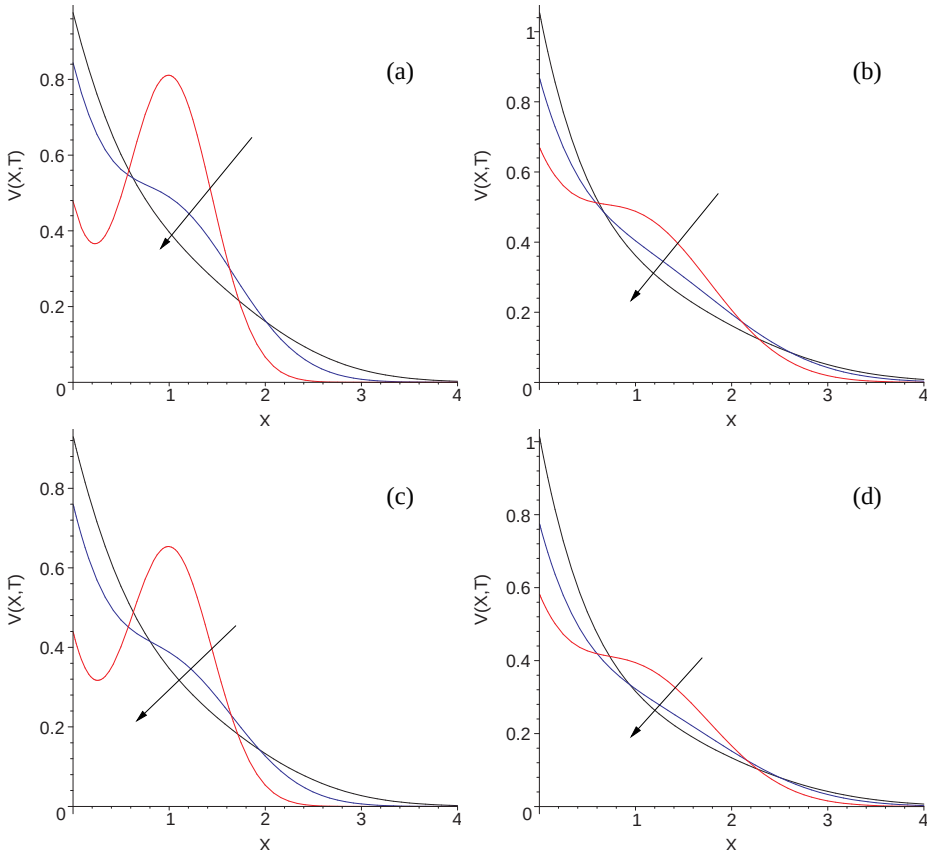

Fig. 8 Plot of the solution, (101), with initial condition $V(X,0)=\delta(X-1)$, and a constant fractional axial current boundary condition with $V_0^{'}=1$, at times $T=0.1$, 0.25, and 0.5 and for (a) $\gamma=1.0$, $\kappa=1.0$, (b) $\gamma=0.5$, $\kappa=1.0$, (c) $\gamma=1.0$, $\kappa=0.5$, and (d) $\gamma=0.5$, $\kappa=0.5$. Time increases in the direction of the arrow.

Case (iii)

The inverse Laplace transform of (88) can be found in a similar fashion to the above cases and the solution to the fractional cable equation, (24), in this case is

$$V(X,T)=\frac{2V_o^{'}T^{\gamma}\,e^{-\mu^2T^{\kappa}}}{\sqrt{4\pi T^{\gamma}}}\sum_{k=0}^{\infty}\frac{\left(\mu^2T^{\kappa}\right)^k}{k!}\Gamma\left(\frac{\kappa}{\gamma}k+1\right)H_{1,2}^{2,0}\left[\frac{x^2}{4T^{\gamma}}\,\middle|\,\begin{matrix}\left(\frac{3}{2}+\frac{\kappa}{\gamma}k,1\right)\\(0,1)\ \ \left(\frac{1}{2},1\right)\end{matrix}\right]$$
$$+\frac{1}{\sqrt{4\pi T^{\gamma}}}e^{-\frac{(X-Y)^2}{4T^{\gamma}}-\mu^2T^{\kappa}}+\frac{1}{\sqrt{4\pi T^{\gamma}}}e^{-\frac{(X+Y)^2}{4T^{\gamma}}-\mu^2T^{\kappa}}. \quad (102)$$

The above solution, (102), for a constant standard axial current boundary condition is very similar to the solution, (101), for a constant fractional axial current boundary condition. The similar behaviours can be seen by comparing the plots in Fig.(8) with those in Fig.(9).

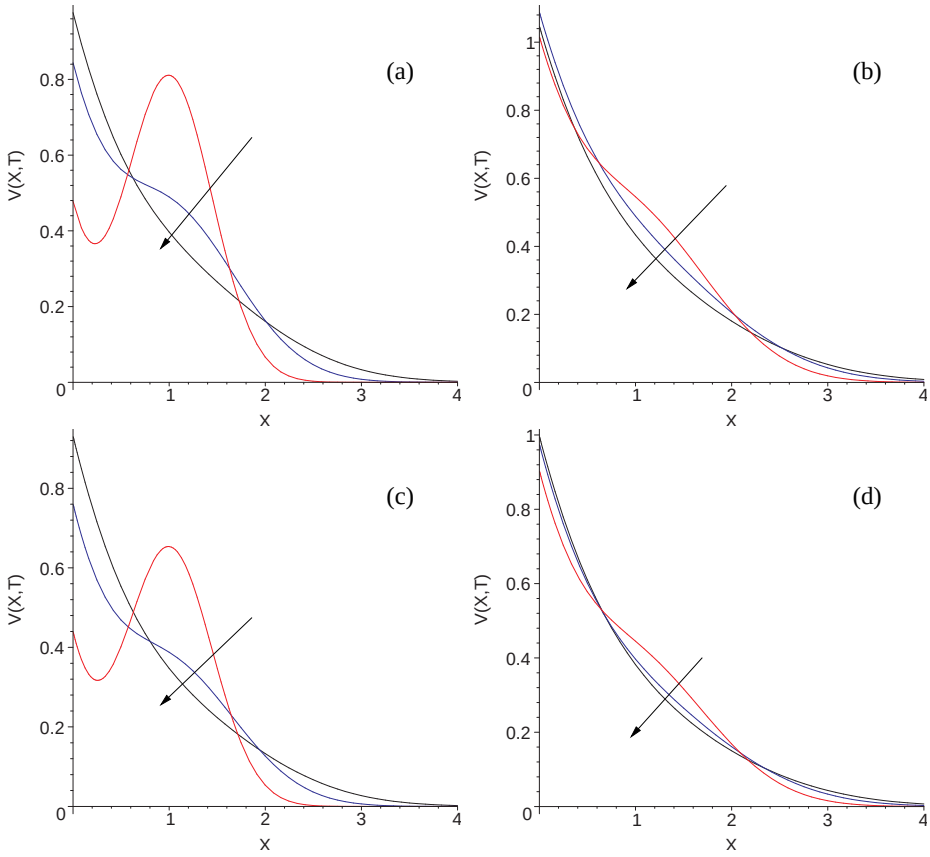

Fig. 9 Plot of the solution, (102), with initial condition $V(X,0) = \delta(X-1)$, and a constant standard axial current boundary condition with $V_0^{'} = 1$, at times $T = 0.1$, 0.25, and 0.5 and for (a) $\gamma = 1.0$, $\kappa = 1.0$, (b) $\gamma = 0.5$, $\kappa = 1.0$, (c) $\gamma = 1.0$, $\kappa = 0.5$, and (d) $\gamma = 0.5$, $\kappa = 0.5$. Time increases in the direction of the arrow.

In the case of standard diffusion, $\gamma = \kappa = 1$, the solution in Case (ii), (101), and the solution in Case (iii), (102), both reduce to

$$V(X,T) = \frac{V_o^{'}}{2\mu}\left[e^{-\mu}\text{Erfc}\left(\sqrt{\frac{X^2}{4T}} - \mu\sqrt{T}\right) - e^{\mu X}\text{Erfc}\left(\sqrt{\frac{X^2}{4T}} + \mu\sqrt{T}\right)\right] + \frac{1}{\sqrt{4\pi T}}e^{-\frac{(X-Y)^2}{4T} - \mu^2 T} + \frac{1}{\sqrt{4\pi T}}e^{-\frac{(X+Y)^2}{4T} - \mu^2 T}. \quad (103)$$

5.2 Semi-Infinite Domain – Model II

The solution of the fractional cable equation, (25), on a semi-infinite domain can also be found using Laplace transform methods (with respect to the time variable T). The Laplace transform of the fractional cable equation, (25), yields

$$\frac{\partial^2 \widehat{V}}{\partial X^2} - \lambda^2(s)\widehat{V} = -s^{\gamma-1}\delta(X-Y) \quad (104)$$

where

$$\lambda(s) = \sqrt{s^{\gamma} + \mu^2 s^{\gamma-\kappa}}$$

and $\widehat{V}$ is the Laplace transform of V. The general solution of this equation is

$$\widehat{V} = A(s)e^{\lambda(s)X} + B(s)e^{-\lambda(s)X} - \frac{s^{\gamma-1}}{\lambda(s)} \begin{cases} 0, & X < Y \\ \sinh\left[\lambda(s)\,(X-Y)\right], & X \geq Y \end{cases} \tag{105}$$

where A and B are arbitrary constants. To ensure the solution is bounded as $X \to \infty$ we require

$$A(s) = \frac{s^{\gamma-1}}{\lambda(s)} \frac{e^{-\lambda(s)Y}}{2}. \tag{106}$$

(105) can then be written as

$$\widehat{V}(X,s) = \frac{s^{\gamma-1}}{2\lambda(s)} e^{-\lambda(s)|X-Y|} + B(s)e^{-\lambda(s)X}. \tag{107}$$

The value of $B(s)$ is determined from the boundary conditions on $V(X,T)$ at $X = 0$. Using the Laplace transform of the boundary conditions in (75)–(77) we obtain the respective solutions in Laplace space:

(i)

$$\widehat{V}(X,s) = \frac{V_o}{s} e^{-\lambda(s)X} + \frac{s^{\gamma-1}}{2\lambda(s)} e^{-\lambda(s)|X-Y|} - \frac{s^{\gamma-1}}{2\lambda(s)} e^{-\lambda(s)(X+Y)}, \tag{108}$$

(ii)

$$\widehat{V}(X,s) = \frac{2V_o^{'}}{s} \frac{s^{\gamma-1}}{2\lambda(s)} e^{-\lambda(s)X} + \frac{s^{\gamma-1}}{2\lambda(s)} e^{-\lambda(s)|X-Y|} + \frac{s^{\gamma-1}}{2\lambda(s)} e^{-\lambda(s)(X+Y)}, \tag{109}$$

(iii)

$$\widehat{V}(X,s) = \frac{2V_o^{'}}{s^{\gamma}} \frac{s^{\gamma-1}}{2\lambda(s)} e^{-\lambda(s)X} + \frac{s^{\gamma-1}}{2\lambda(s)} e^{-\lambda(s)|X-Y|} + \frac{s^{\gamma-1}}{2\lambda(s)} e^{-\lambda(s)(X+Y)}. \tag{110}$$

Note in each case the last two terms are the Laplace transform of $G(X-Y,T)$ and $G(X+Y,T)$ respectively where $G(X,T)$ is the infinite domain solution in (46) and thus it remains to find the inverse transform of the first term which we do on a case by case basis below.

Case (i)

In order to invert the term

$$\widehat{\phi}_1(s) = \frac{V_o}{s} e^{-\lambda(s)X} = \frac{V_o}{s} e^{-Xs^{\frac{\gamma}{2}}\sqrt{1+\mu^2 s^{-\kappa}}} \tag{111}$$

we first consider the related function

$$g(z) = e^{-\rho\sqrt{z}} = H_{0,1}^{1,0}\left[\rho z^{\frac{1}{2}} \,\middle|\, \begin{matrix} - \\ (0,1) \end{matrix}\right] \tag{112}$$

where ρ and z are defined in (37) and (38). The function $g(z)$ can be written as a series expansion in Fox functions as follows

$$g(z) = \sum_{k=0}^{\infty} g^{(k)}(1)\frac{(z-1)^k}{k!} = \frac{1}{\sqrt{\pi}} \sum_{k=0}^{\infty} (-1)^k \frac{(z-1)^k}{k!} H_{0,2}^{2,0}\left[\frac{\rho^2}{4} \,\middle|\, \begin{matrix} - \\ \left(\frac{1}{2},1\right)\,(k,1) \end{matrix}\right]. \tag{113}$$

Thus we have

$$\widehat{\phi}_1(s) = \frac{V_0}{\sqrt{\pi}} \sum_{k=0}^{\infty} \frac{\left(-\mu^2\right)^k}{k!} s^{-k\kappa-1} H_{0,2}^{2,0}\left[\frac{x^2 s^\gamma}{4} \middle| \begin{matrix} - \\ \left(\frac{1}{2},1\right)\ (k,1) \end{matrix} \right]. \tag{114}$$

which can also be written, using the reduction formula given in (168) with $d = 1+\kappa k$ and $\Delta = \gamma$, as

$$\widehat{\phi}_1(s) = \frac{V_0}{\sqrt{\pi}} \sum_{k=0}^{\infty} \frac{\left(-\mu^2\right)^k}{k!} s^{-k\kappa-1} H_{1,3}^{3,0}\left[\frac{x^2 s^\gamma}{4} \middle| \begin{matrix} (1+\kappa k,\gamma) \\ (1+\kappa k,\gamma)\ \left(\frac{1}{2},1\right)\ (k,1) \end{matrix} \right]. \tag{115}$$

We can now identify each term of (115) as a Laplace transform of a Fox function using (169) with $\omega = k\kappa$, $\sigma = \gamma$, and $z = x^2/4$ so that we obtain

$$\phi_1(T) = \frac{V_o}{\sqrt{\pi}} \sum_{k=0}^{\infty} \frac{\left(-\mu^2 T^\kappa\right)^k}{k!} H_{1,2}^{2,0}\left[\frac{x^2}{4T^\gamma} \middle| \begin{matrix} (1+\kappa k,\gamma) \\ \left(\frac{1}{2},1\right)\ (k,1) \end{matrix} \right]. \tag{116}$$

The solution of the fractional cable equation, (25), that now follows from .(108), (111), (37), (38), (116) in this case is given by

$$V(X,T) = \frac{V_o}{\sqrt{\pi}} \sum_{k=0}^{\infty} \frac{\left(-\mu^2 T^\kappa\right)^k}{k!} H_{1,2}^{2,0}\left[\frac{X^2}{4T^\gamma} \middle| \begin{matrix} (1+\kappa k,\gamma) \\ \left(\frac{1}{2},1\right)\ (k,1) \end{matrix} \right] + G(X-Y,T) - G(X+Y,T) \tag{117}$$

with $G(X,T)$ given by (46). In the case of standard diffusion this solution reduces to the result in (97).

In Fig 10 we show the plot of the solution, (117), for different values of γ and κ with $V_0 = 1$ and $V(X,0) = \delta(X-1)$. Note that when $\gamma = 1$ (first column) the derivative is continuous at $X = 1$ in contrast to when $\gamma = 0.5$ (second column).

Case (ii)

In (109) the first term

$$\widehat{\phi}_2(s) = \frac{2V_o^{'}}{s} \frac{s^{\gamma-1}}{2\lambda(s)} e^{-\lambda(s)x} \tag{118}$$

can be inverted by noting the relation, in Laplace space, with an integral of the infinite domain solution given in (46). The Laplace transform of the infinite domain solution is

$$\mathscr{L}\left\{G(X,T)\right\}(s) = \frac{s^{\gamma-1}}{2\lambda(s)} e^{-\lambda(s)X} \tag{119}$$

so that we can write

$$\widehat{\phi}_2(s) = 2V_o^{'} \mathscr{L}\left\{ \int_0^T G\left(X,t^{'}\right) dt^{'} \right\}(s) \tag{120}$$

which upon inverting gives

$$\phi_2(T) = 2V_o^{'} \int_0^T G\left(X,t^{'}\right) dt^{'}. \tag{121}$$

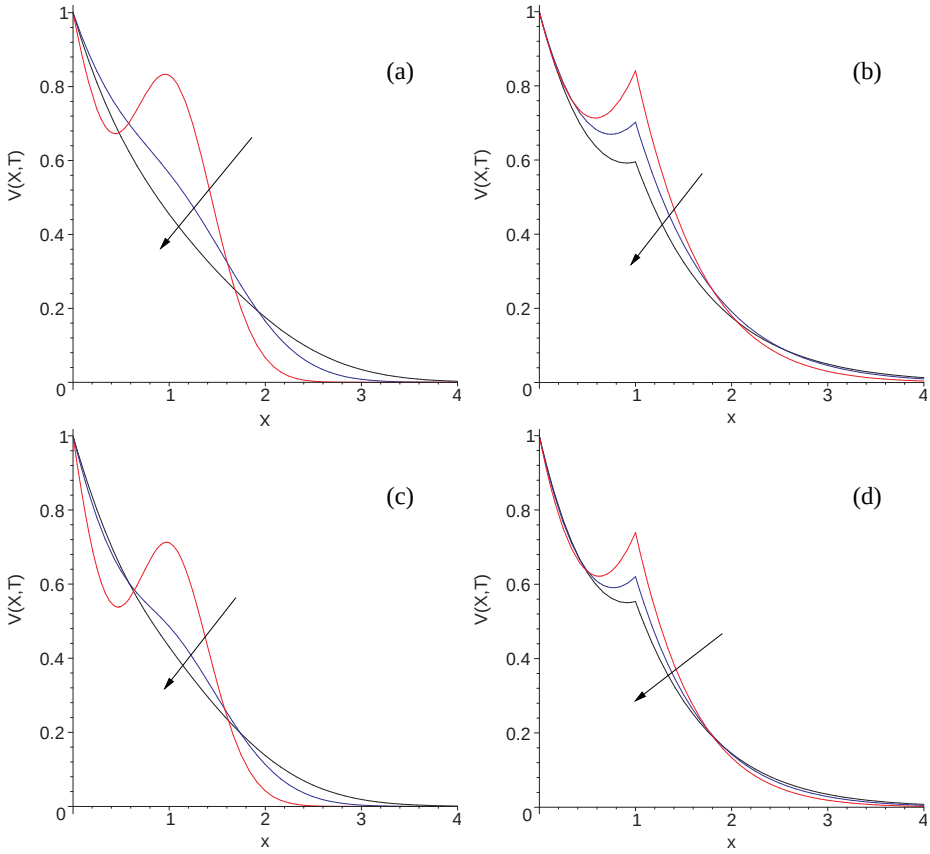

Fig. 10 Plot of the potential in the semi-infinite cable, Model II, with initial condition $V(X,0) = \delta(X-1)$ and the fixed value boundary condition $V_0 = 1$. The solution is shown at $T = 0.1$, 0.25, and 0.5 for the case of (a) $\gamma = 1.0, \kappa = 1$, (b) $\gamma = 0.5, \kappa = 1.0$, (c) $\gamma = 1.0, \kappa = 0.5$, and (d) $\gamma = 0.5, \kappa = 0.5$. Time increases in the direction of the arrow.

The above expression can be evaluated as a series expansion in Fox functions by using (46) and (164) with $\beta = -\gamma$, $\alpha = -\gamma/2 + \kappa n$ and $\nu = -1$. The corresponding semi-infinite solution of the fractional cable equation in this case is now

$$V(X,T) = \frac{2V_o' T}{\sqrt{4\pi T^\gamma}} \sum_{k=0}^{\infty} \frac{\left(-\mu^2 t^\kappa\right)^k}{k!} H_{1,2}^{2,0}\left[\frac{X^2}{4T^\gamma} \middle| \begin{matrix} \left(2 - \frac{\gamma}{2} + \kappa k, \gamma\right) \\ (0,1)\ \left(\frac{1}{2} + k, 1\right) \end{matrix} \right] + G(X-Y,T) + G(X+Y,T). \quad (122)$$

This solution is plotted in Fig 11 for different values of γ and κ with $V_0' = 1$ and $V(X,0) = \delta(X-1)$. Note when $\gamma = 1$ (first column) the derivative is again continuous in contrast to the cases with anomalous subdiffusion ($\gamma = 0.5$ in the second column).

Case (iii)

In (109) the first term

$$\widehat{\phi}_3(s) = \frac{2V_o^{'}}{s^{\gamma}} \frac{s^{\gamma-1}}{2\lambda(s)} e^{-\lambda(s)x} \tag{123}$$

can be identified as a fractional integral of the infinite domain solution in Laplace space, i.e.,

$$\widehat{\phi}_3(s) = 2V_o^{'} \mathscr{L}\left\{ \frac{\partial^{-\gamma}}{\partial T^{-\gamma}} G(X,T) \right\}(s). \tag{124}$$

This can now be inverted to obtain

$$\phi_3(T) = 2V_o^{'} \frac{\partial^{-\gamma}}{\partial T^{-\gamma}} G(X,T), \tag{125}$$

and the resulting expression can be evaluated as a series expansion in Fox functions by using (46) and (164) with $\beta = -\gamma$, $\alpha = -\gamma/2 + \kappa n$ and $\nu = -\gamma$.

The semi-inifinite domain solution in this case is given by

$$V(X,T) = \frac{2V_o^{'} T^{\gamma}}{\sqrt{4\pi T^{\gamma}}} \sum_{k=0}^{\infty} \frac{\left(-\mu^2 T^{\kappa}\right)^k}{k!} H_{1,2}^{2,0}\left[\frac{X^2}{4T^{\gamma}} \,\middle|\, \begin{matrix} \left(1+\frac{\gamma}{2}+\kappa k, \gamma\right) \\ (0,1)\ \left(\frac{1}{2}+k, 1\right) \end{matrix} \right] + G(X-Y,T) + G(X+Y,T), \tag{126}$$

with $G(X,T)$ given in (46). This solution is plotted in Fig.12 for different values of γ and κ with $V_o^{'} = 1$ and $V(X,0) = \delta(X-1)$.

In the case of standard diffusion, the two solutions, (122) and (126), both reduce to (103).

Overall the semi-infinite domain solutions with pulse initial conditions $V(X,0) = \delta(X-1)$ are broadly similar to the case where diffusion is standard along the axial direction of the cable. In both Model I and Model II, with different values of κ and different boundary conditions at $X = 0$, the initial pulse at $X = 1$ decays and the long time plot of $V(X,T)$ is approximately exponential. When the diffusion is anomalous along the axial direction of the cable the initial pulse decays faster in Model I whereas in Model II the initial decay is fast but the long time decay is slow and the pulse at $X = 1$ is non-differentiable at subsequent times.

6 Action Potential Firing Rates

Firing rates can be deduced from the fractional cable equations by using a simple passive leaky integrate-and-fire model [7] based on solutions with $\dfrac{\partial^2 V}{\partial X^2} = 0$ for a homogenous membrane patch, and with a constant externally applied current density i_e.

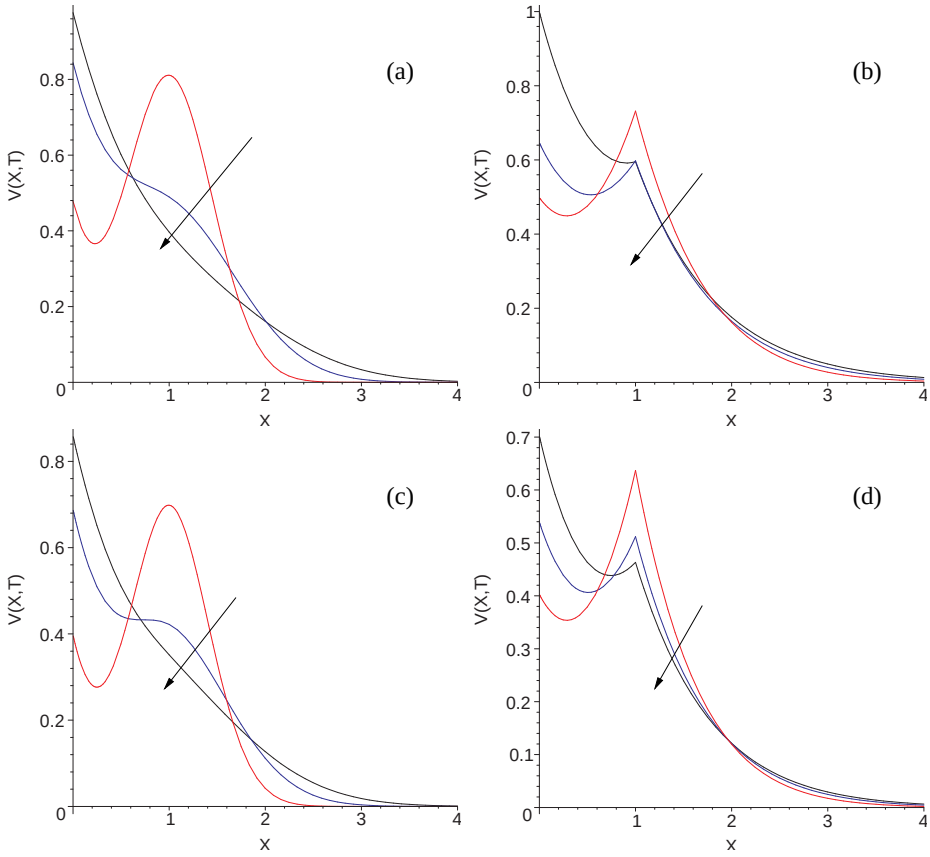

Fig. 11 Plot of the potential in the semi-infinite cable, Model II, with initial condition $V(X,0) = \delta(X-1)$ and a constant fractional axial current boundary condition with $V_0^{'} = 1$. The solution is shown at $T = 0.1$, 0.25, and 0.5 for the case of (a) $\gamma = 1.0, \kappa = 1$, (b) $\gamma = 0.5, \kappa = 1.0$, (c) $\gamma = 1.0, \kappa = 0.5$, and (d) $\gamma = 0.5, \kappa = 0.5$. Time increases in the direction of the arrow.

6.1 Firing Rates – Model I

Starting with the dimensionless fractional cable equation, (24), and setting $\dfrac{\partial^2 V}{\partial X^2} = 0$ we have

$$\frac{\partial V}{\partial T} = -\mu^2 \kappa T^{\kappa-1} \left(V - i_e r_m\right), \tag{127}$$

with solution

$$V(T) = i_e r_m + \left(V_0 - i_e r_m\right) e^{-\mu^2 T^\kappa}. \tag{128}$$

The time for the potential to increase from an initial reset value, $V_0 = V_{reset}$, to a threshold value for firing, $V(T_f) = V_{th}$, can readily be obtained by solving (128) for T_f. The result is

$$T_f = \left(\frac{1}{\mu^2} \ln\left(\frac{1}{\rho}\right)\right)^{\frac{1}{\kappa}} \tag{129}$$

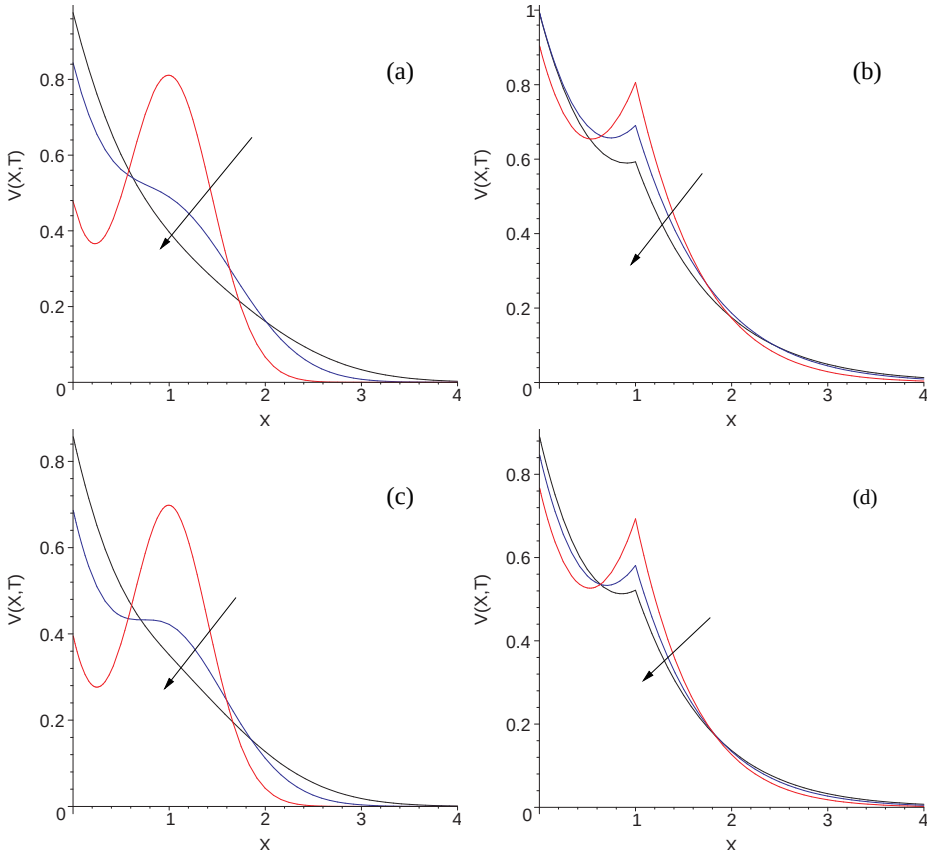

Fig. 12 Plot of the potential in the semi-infinite cable, Model II, with initial condition $V(X,0) = \delta(X-1)$ and and a constant standard axial current boundary condition with $V_0^{'} = 1$. The solution is shown at $T = 0.1$, 0.25, and 0.5 for the case of (a) $\gamma = 1.0, \kappa = 1$, (b) $\gamma = 0.5, \kappa = 1.0$, (c) $\gamma = 1.0, \kappa = 0.5$, and (d) $\gamma = 0.5, \kappa = 0.5$. Time increases in the direction of the arrow.

where

$$\rho = \frac{V_{th} - i_e r_m}{V_{reset} - i_e r_m}. \tag{130}$$

The firing rate τ is the reciprocal of the firing time,

$$\tau_I = \left(\frac{1}{\mu^2} \ln\left(\frac{1}{\rho} \right) \right)^{-\frac{1}{\kappa}}. \tag{131}$$

Positive solutions for the firing rate can only be obtained if $0 < \rho \leq 1$. This defines the same cut-off rheobase current $i_e > V_{th}/r_m$ as the standard leaky integrate and fire model. However the firing rate, (131) in the fractional integrate and fire model is affected by the fractional scaling exponent κ through the dependence on μ, (28). If $\rho < e^{-\mu^2}$ the firing rate is a monotonic increasing function of κ whereas if $\rho > e^{-\mu^2}$ it is a monotonic decreasing function. In the special case where $\rho = e^{-\mu^2}$ the firing rate is constant with respect κ. The firing rate, (131) is plotted in Fig 13 as a function of κ for different values of ρ.

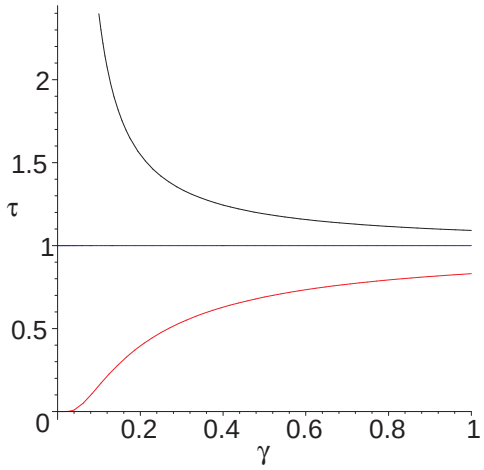

Fig. 13 Plots of the firing rate, τ, as a function of the exponent κ in the case of Model I for parameters $\rho = 0.3$ (red lower), $\rho = e^{-1}$ (blue middle) and $\rho = 0.4$ (black upper). Here we have set $\mu = 1$.

6.2 Firing Rates – Model II

Starting with the dimensionless fractional cable equation for Model II, (25), and setting $\dfrac{\partial^2 V}{\partial X^2} = 0$ we have

$$\frac{\partial V}{\partial T} = -\mu^2 \frac{\partial^{1-\kappa}}{\partial T^{1-\kappa}} (V - i_e r_m) . \tag{132}$$

This equation has solution

$$V(T) = i_e r_m + (V_0 - i_e r_m) E_\kappa \left(-\mu^2 T^\kappa\right) \tag{133}$$

where V_0 is the initial potential and $E_\kappa(z)$ is the Mittag-Leffler function, [27], which behaves like a stretched exponential

$$E_\kappa \left(-\mu^2 T^\kappa\right) \sim \exp\left(-\frac{\mu^2 T^\kappa}{\Gamma(1+\kappa)}\right) \tag{134}$$

for small times and decays to zero like an inverse power law for long times [24]. It follows that the solution reaches a steady state given by $V = i_e r_m$. Incorporating the results from (133) and (134) in a simple passive leaky integrate-and-fire model [7] now yields the firing rate

$$\tau_{II} \sim \left[\frac{\Gamma(1+\kappa)}{\mu^2} \ln\left(\frac{1}{\rho}\right)\right]^{-\frac{1}{\kappa}} . \tag{135}$$

with ρ defined in (130). Again this model predicts the same cut-off rheobase current as the standard leaky integrate and fire model. However the firing rate, (135), in the fractional leaky integrate and fire model is affected by the scaling exponent κ as follows: For a fixed value of $\rho \gg 0.5$ the firing rate increases with decreasing κ whereas for $\rho \ll 0.5$ the firing rate decreases with decreasing κ. There is little variation in the firing rate with κ in the intermediate regime $\rho \approx 0.5$.

7 Calibration and Validation

An experimental measurement of voltage attenuation is provided by the ratio of the peak potential at the soma to the peak potential at different points along the dendrite in response to an alpha function input along the dendrite [11]. Standard cable theory predicts exponential steady state voltage attenuation. In Figure 14 (Model I) and Figure 15 (Model II), we show log-linear plots of the ratio

$$\rho^*(X) = \frac{\max_T [V_{soma}(T)]}{\max_T [V(X,T)]} \tag{136}$$

for various input positions X_0 along the dendrite, and for different values of γ and κ. The peak potentials used to calculate ρ^* were obtained from (63) (Model I) and (74) (Model II).

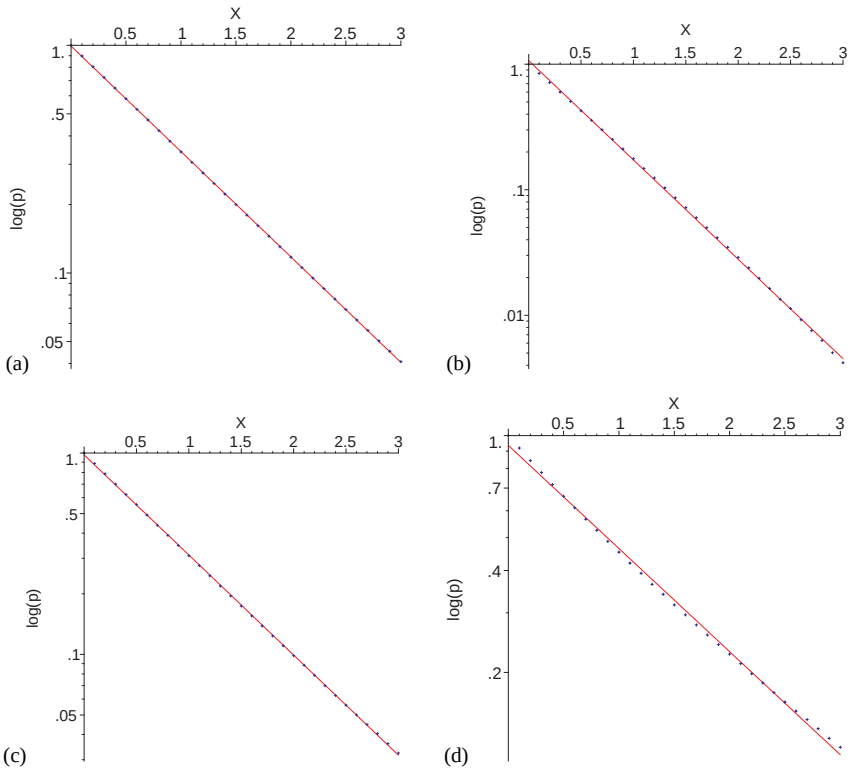

Fig. 14 Log-linear plot of ρ^* versus X for Model I (24), with an alpha function input and parameters (a) $\gamma = 1.0, \kappa = 1.0$, (b) $\gamma = 0.5, \kappa = 1.0$ (c) $\gamma = 1.0, \kappa = 0.5$ (d) $\gamma = 0.5, \kappa = 0.5$ The other parameters are $\alpha = \mu = \beta = 1$. The straight line of best fit is also shown.

For each set of parameters the voltage attenuation can be well approximated by an exponential fit, however the slopes estimated from the log-linear plots differ for the different parameters sets and the different models (see Table 1).

It follows that exponential voltage attenuation is not a discriminating feature of standard cable theory and cable properties cannot be inferred from such experiments without additional information. A further difficulty in making comparisons with experiments is that the results shown are in dimensionless variables. In particular, the input position, X_0, is in terms

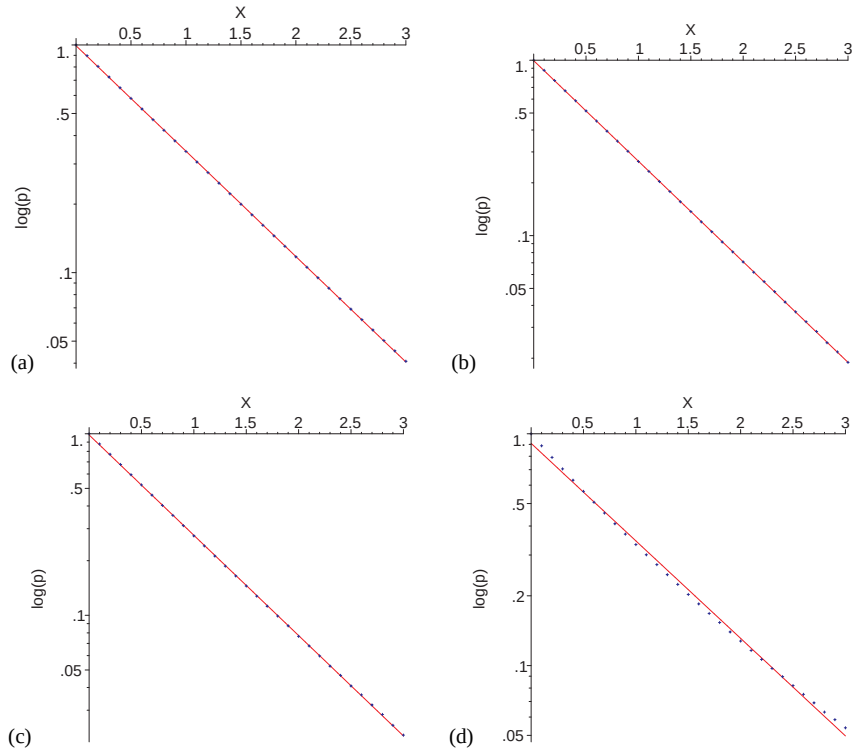

Fig. 15 Log-linear plot of ρ^* versus X for Model II (25), with an alpha function input and parameters (a) $\gamma = 1.0, \kappa = 1.0$, (b) $\gamma = 0.5, \kappa = 1.0$ (c) $\gamma = 1.0, \kappa = 0.5$ (d) $\gamma = 0.5, \kappa = 0.5$ The other parameters are $\alpha = \mu = \beta = 1$. The straight line of best fit is also shown.

Table 1 Slopes of straight lines of best fit in log-linear plots of $\rho^*(X)$ versus X for different values of the fractional exponents γ and κ.

Parameters	Slope	
	Model I	Model II
$\gamma = 1.0, \kappa = 1.0$	-1.066	-1.066
$\gamma = 0.5, \kappa = 1.0$	-1.822	-1.320
$\gamma = 0.5, \kappa = 0.5$	-1.144	-1.272
$\gamma = 1.0, \kappa = 0.5$	-0.701	-0.968

of the dimensionless space variable, (27), which is itself a function of γ, r_m, c_m, r_L, d. Additional information could be obtained from patch clamp recordings in response to prescribed current inputs. For example in the case of a constant current input, the parameters r_m, μ, κ could be obtained from fits based on (128) and (133) Assuming standard values for c_m and assuming that $\gamma = \kappa$ in steady state, estimates of $r_L(\gamma)$ could then be obtained from voltage attenuation measurements using simultaneous patch-pipette recordings [47] from the soma and the apical dendrite of a pyramidal tree.

8 Discussion

The fractional cable equations described in this paper could be used to model electrical signalling properties of nerve cells with anomalous electrodiffusion due to trapping or macromolecular crowding. Important examples where this could find application include (i) spiny dendrites, in which the trapping and release of molecules by spines results in anomalous diffusion on mesoscopic time scales along the axial direction of nerve cells and (ii) dendrites with intracellular plaques where macromolecular crowding effects result in anomalous diffusion. The results in this paper show how the scaling exponents of the anomalous diffusion impact on the electrotonic properties of dendrites and on action potential firing rates. However the results in this paper are just a first step. In order to make detailed comparisons with real nerve cells it will be necessary to extend the fractional cable results to finite domains and to compartment models. Work on this is in progress.

Acknowledgements This research was supported by the Australian Commonwealth Government ARC Discovery Grants Scheme and USA NIH Grants DC05669 and MH071818.

References

1. Banks, D.S., Fradin, C.: Anomalous diffusion of proteins due to molecular crowding. Biophys. J **89**, 2960–2971 (2005)
2. Barkai, E., Cheng, Y.C.: Aging continuous time random walks. J. Chemical Phys. **118**, 6167–6178 (2003)
3. Barkai, E., Metzler, R., Klafter, J.: From continuous time random walks to the fractional Fokker-Planck equation. Phys. Rev. E **61**, 132–138 (2000)
4. Braaksma, B.: Asymptotic expansions and analytic continuations for a class of Barnes-integrals. Compositio. Math. **15**, 239–341 (1963)
5. Brown, E.B., Wu, E.S., Zipfel, W., Webb, W.W.: Measurement of molecular diffusion in solution by multiphoton fluorescence photobleaching recovery. Biophys. J. **77**, 2837–2849 (1999)
6. Compte, A., Metzler, R.: The generalized Cattaneo equation for the description of anomalous transport processes. J. Phys. A: Math. Gen. **30**, 7277–7289 (1997)
7. Dayan, P., Abbott, L.F.: Theoretical Neuroscience: Computational and Mathematical Modeling of Neural Systems. MIT Press, Cambridge, Massachusetts (2001)
8. Feder, T.J., Brust-Mascher, I., Slattery, J.P., Baird, B., Webb, W.W.: Constrained diffusion or immobile fraction on cell surfaces: A new interpretation. Biophys. J. **70**, 2767–2773 (1996)
9. Furini, S., Zerbetto, F., Cavalcanti, S.: Application of the Poisson-Nernst-Planck theory with space dependent diffusion coefficients to KcsA. Biophys. J. **91**, 3162–3169 (2006)
10. Gabso, M., Neher, E., Spira, M.: Low mobility of Ca^{2+} buffers in axons of cultured aplysia neurons. Neuron **18**, 473–481 (1997)
11. Golding, N., Mickus, T., Katz, Y., Kath, W., Spruston, N.: Factors mediating powerful voltage attenuation along CA1 pyramidal neuron dendrites. J. Physiology **568**, 69–82 (2005)
12. Goychuk, I., Hänggi, P.: Fractional diffusion modelling of ion channel gating. Phys. Rev. E **70**, 051,915 (2004)
13. Guigas, G., Kalla, C., Weiss, M.: The degree of macromolecular crowding in the cytoplasm and nucleoplasm of mammalian cells is conserved. FEBS Letters **581**, 5094–5098 (2007)
14. Heinsalu, E., Patriarca, M., Goychuk, I., Hänggi, P.: Use and abuse of a fractional Fokker-Planck dynamics for time-dependent driving. Phys. Rev. Lett. **99**, 120,602 (2007)
15. Henry, B.I., Langlands, T.A.M., Wearne, S.L.: Anomalous diffusion with linear reaction kinetics: From continuous time random walks to fractional reaction-diffusion equations. Phys. Rev. E **74**, 031,116 (2006)
16. Henry, B.I., Langlands, T.A.M., Wearne, S.L.: Fractional cable models for spiny neuronal densites. Phys. Rev. Letts. **100**, 128,103 (2008)
17. Henry, B.I., Wearne, S.L.: Fractional reaction-diffusion. Physica A **276**, 448–455 (2000)
18. Hille, B.: Ionic Channels of Excitable Membranes. Sinauer Associates Inc, Massachusetts (1984)
19. Koeller, R.C.: Applications of fractional calculus to the theory of viscoelasticity. J. Appl. Mech. **51**, 299–307 (1984)

20. Langlands, T.A.M., Henry, B.I., Wearne, S.L.: Anomalous subdiffusion with multispecies linear reaction dynamics. Phys. Rev. E. **77**, 021,111 (2008)
21. Lutz, E.: Fractional Langevin equation. Phys. Rev. E **64**, 051,106 (2001)
22. Mathai, A.M., Saxena, R.K.: The *H*-Functions with Applications in Statistics and Other Disciplines. Wiley Eastern Ltd, New Delhi (1978)
23. Metzler, R., Barkai, E., Klafter, J.: Deriving fractional Fokker-Planck equations from a generalised master equation. Europhys Letts **46**, 431 (1999)
24. Metzler, R., Klafter, J.: The random walk's guide to anomalous diffusion: A fractional dynamics approach. Phys. Rep. **339**, 1–77 (2000)
25. Nonner, W., Eisenberg, B.: Ion permeation and glutamate residues linked by Poisson-Nernst Planck theory in l-type calcium channels. Biophysics Journal **75**, 1287–1305 (1998)
26. Podlubny, I.: The Laplace transform method for linear differential equations of the fractional order. UEF 02-94, Slovak Academy of Sciences Institute of Experimental Physics (1994)
27. Podlubny, I.: Fractional differential equations, *Mathematics in Science and Engineering*, vol. 198. Academic Press, New York and London (1999)
28. Qian, N., Sejnowski, T.: An electro-diffusion model for computing membrane potentials and ionic concentrations in branching dendrites, spines and axons. Biol. Cybern. **62**, 1–15 (1989)
29. Rall, W.: Branching dendritic trees and motoneuron membrane resistivity. Exp. Neurol. **1**, 491–527 (1959)
30. Rall, W.: Core conductor theory and cable properties of neurons. In: R. Poeter (ed.) Handbook of Physiology: The Nervous System, vol. 1, pp. 39–97. American Physiological Society, Bethesda, Md (1977). Chapter 3
31. Reynolds, A.: On the anomalous diffusion characteristics of membrane bound proteins. Phys. Lett. A **342**, 439–442 (2005)
32. Ritchie, K.: Detection of non-Browian diffusion in the cell membrane in single molecure tracking. Biophys. J. **88**, 2266–2277 (2005)
33. Santamaria, F., Wils, S., De Schutter, E., Augustine, G.J.: Anomalous diffusion in purkinje cell dendrites caused by spines. Neuron **52**, 635–648 (2006)
34. Saxton, M.J.: Anomalous diffusion due to obstacles: A Monte Carlo Study. Biophys. J. **66**, 394–401 (1994)
35. Saxton, M.J.: Anomalous diffusion due to binding: A Monte Carlo Study. Biophys. J. **70**, 1250–1262 (1996)
36. Saxton, M.J.: Anomalous subdiffusion in fluorescence photobleaching recovery: A Monte Carlo study. Biophys. J. **81**, 2226–2240 (2001)
37. Scher, H., Montroll, E.W.: Anomalous transit-time dispersion in amorphous solids. Phys. Rev. B. **12**, 2455–2477 (1975)
38. Schnell, S., Turner, T.E.: Reaction kinetics in intracellular environments with macromolecular crowding: simulations and rate laws. Prog. Biophys. Mol. Biol. **85**, 235–260 (2004)
39. Sheets, E.D., Lee, G.M., Simson, R., Jacobson, K.: Transient confinement of a glycosylphosphatidylinositol-anchored protein in the plasma membrane. Biochem. **36**, 12,449–12,458 (1997)
40. Simson, R., Yang, B., Moore, S.E., Doherty, P., Walsh, F.S., Jacobson, K.A.: Structural mosaicism on the submicron scale in the plasma membrane. Biophys. J. **74**, 297–308 (1998)
41. Smith, P.R., Morrison, I.E.G., Wilson, K.M., Fernandez, N., Cherry, R.J.: Anomalous diffusion of major histocompatability complex class I molecules on HeLa cells determined by single particle tracking. Biophys. J. **76**, 3331–3344 (1999)
42. Sokolov, I., Blumen, A., Klafter, J.: Linear response in complex systems: CTRW and the fractional fokker-planck equations. Physica A **302**, 268–278 (2001)
43. Sokolov, I.M.: Thermodynamics and fractional Fokker-Planck equations. Phys. Rev. E **63**, 056,111 (2001)
44. Sokolov, I.M., Klafter, J.: Field-Induced Dispersion in Subdiffusion. Phys. Rev. Lett. **97**, 140,602 (2006)
45. Sokolov, I.M., Schmidt, M.G.W., Sagues, F.: Reaction-subdiffusion equations. Phys. Rev. E **73**, 031,102 (2006)
46. Srivastava, H., Gupta, K., Goyal, S.: The *H*-Functions of One and Two Variables with Applications. South Asian Publishers Pvt Ltd, New Delhi (1982)
47. Stuart, G., Spruston, N.: Determinants of voltage attenuation in neocortical pyramidal neuron dendrites. The Journal of Neuroscience **18**, 3501–3510 (1998)
48. Trigger, S.A., van Heijst, G.J.F., Petrov, O.F., Schram, P.P.J.M.: Diffusion in a time-dependent field. Phys. Rev. E **77**, 011,107 (2008)
49. Tuckwell, H.: Introduction to theoretical neurobiology, vol. 1. Cambridge University Press, Cambridge, UK (1988)

50. Wachsmuth, M., Weidemann, T., Müller, G., Hoffmann-Rohrer, U., Knoch, T., Waldeck, W., Langowski, J.: Analyzing intracellular binding and diffusion with continuous fluorescence photobleaching. Biophys. J. **84**, 3353–3363 (2003)
51. Wang, K.G.: Long-time correlation effects and biased anomalous diffusion. Phys. Rev. A. **45**, 833–837 (1992)
52. Wang, K.G.: Long-range correlation effects, generalized Brownian motion and anomalous diffusion. J. Phys. A **27**, 3655–3661 (1994)
53. Wang, K.G., Lung, C.W.: Long-time correlation effects and fractal Brownian motion. Phys. Letts. A **151**, 119–121 (1999)
54. Weiss, M., Elsner, M., Kartberg, F., Nilsson, T.: Anomalous Subdiffusion is a Measure for Cytoplasmic Crowding in Living Cells. Biophys. J. **87**, 3518–3524 (2004)
55. Weron, A., Magdziarz, M., Weron, K.: Modeling of subdiffusion in space-time-dependent force fields beyond the fractional Fokker-Planck equation. Phys. Rev. E. **77**, 036,704 (2008)
56. Zanette, D.: Macroscopic current in fractional anomalous diffusion. Physica A **252**, 159–164 (1998)

A Equal Exponents

In this appendix we explore the relationships between solutions of the fractional cable equations, (24) and (25), for equal values of the scaling exponents, $\gamma = \kappa$, and solutions of the standard cable equation

$$\frac{\partial V}{\partial T} = \frac{\partial^2 V}{\partial X^2} - V. \tag{137}$$

For comparison purposes we denote the solutions of the standard cable equation by $V(X,T)$, the solutions of Model I by $V_I(X,T)$ and the solutions of Model II by $V_{II}(X,T)$. The fundamental solution of the standard cable equation is

$$G(X,T) = \frac{1}{\sqrt{4\pi T}} e^{-\frac{X^2}{4T} - T}. \tag{138}$$

To simplify the algebra we have set $\mu = 1$ in the following.

A.1 Model I

The solutions of the fractional cable equation, Model I, with equal exponents are identical to the solutions of the standard cable equations except that they occur on a slower time scale, T^γ. To see this we observe that the fractional cable equation

$$\frac{\partial V_I}{\partial T} = \gamma T^{\gamma-1} \frac{\partial^2 V_I}{\partial X^2} - \mu^2 \gamma T^{\gamma-1} V_I, \tag{139}$$

can be simplified by introducing the change of variables

$$S = T^\gamma \tag{140}$$

with

$$U(X,S) = V_I(X,T). \tag{141}$$

The equation for $U(X,S)$ is the standard cable equation and thus

$$V_I(X,T) = V(X,T^\gamma). \tag{142}$$

In particular the fundamental solution is

$$G_I(X,T) = \frac{1}{\sqrt{4\pi T^\gamma}} e^{-\frac{X^2}{4T^\gamma} - T^\gamma}. \tag{143}$$

A.2 Model II

The solutions of the fractional cable equation, Model II, with equal exponents are time subordinated to the solutions of the standard cable equations. Explicitly it can be shown that

$$V_{II}(X,T) = \int_0^\infty V(X,\tau)\phi(\tau,T)\,d\tau \tag{144}$$

where $\phi(\tau,T)$ is a Levy stable subordinator with Laplace transform

$$\hat{\phi}(\tau,s) = \int_0^\infty \phi(\tau,T)e^{-sT}\,dT. \tag{145}$$

$$= s^{\gamma-1}e^{-\tau s^\gamma} \tag{146}$$

The variable τ defines an operational time that is distinct from the physical time T.

Starting with the fractional cable equation,

$$\frac{\partial V_{II}}{\partial T} = \frac{\partial^{1-\gamma}}{\partial T^{1-\gamma}}\frac{\partial^2 V_{II}}{\partial X^2} - \frac{\partial^{1-\gamma}}{\partial T^{1-\gamma}}V_{II}, \tag{147}$$

we take the Laplace transform with respect to T to obtain

$$s\hat{V}_{II}(X,s) - V_{II}(X,0) = s^{1-\gamma}\frac{\partial^2 \hat{V}_{II}(X,s)}{\partial X^2} - s^{1-\gamma}\hat{V}_{II}(X,s). \tag{148}$$

But, using (146) we can write

$$\hat{V}_{II}(X,s) = s^{\gamma-1}\int_0^\infty V(X,\tau)e^{-\tau s^\gamma}\,d\tau \tag{149}$$

$$= s^{\gamma-1}\hat{V}(X,s^\gamma), \tag{150}$$

and then using (150) in (148) we have

$$s^\gamma\hat{V}(X,s^\gamma) - V(X,0) = \frac{\partial^2\hat{V}(X,s^\gamma)}{\partial X^2} - \hat{V}(X,s^\gamma) \tag{151}$$

where we have assumed that

$$V_{II}(X,0) = V(X,0).$$

Finally we take the inverse Laplace transform of (151) with respect to the variable s^γ to obtain the governing evolution equation for $V(X,T)$:

$$\frac{\partial V}{\partial T} = \frac{\partial^2 V}{\partial X^2} - V, \tag{152}$$

which is the standard cable equation.

The result in (144) with the Laplace transform of $\phi(\tau,T)$ defined by (146) can also be shown directly. We first note that the inverse Laplace transform of (146) can be evaluated as a Fox function as follows

$$\phi(\tau,T) = \frac{1}{T^\gamma}H_{1,1}^{1,0}\left[\frac{\tau}{T^\gamma}\middle|\begin{matrix}(1-\gamma,\gamma)\\(0,1)\end{matrix}\right]. \tag{153}$$

If we subsitute the above expression into (144) using the fundamental solution for $V(X,T)$ in (138) we obtain

$$V_{II}(X,T) = \int_0^\infty \frac{1}{T^\gamma}H_{1,1}^{1,0}\left[\frac{\tau}{T^\gamma}\middle|\begin{matrix}(1-\gamma,\gamma)\\(0,1)\end{matrix}\right]\frac{1}{\sqrt{4\pi\tau}}e^{-\frac{X^2}{4\tau}-\tau}\,d\tau \tag{154}$$

We now introduce a change of variables

$$\omega = \frac{\tau}{T^\gamma} \tag{155}$$

to obtain

$$V_{II}(X,T) = \frac{1}{4\pi T^\gamma}\int_0^\infty H_{1,1}^{1,0}\left[\omega\middle|\begin{matrix}(1-\gamma,\gamma)\\(0,1)\end{matrix}\right]\frac{e^{-\frac{\theta}{\omega}-\beta\omega}}{\sqrt{\omega}}\,d\omega \tag{156}$$

where

$$\theta = \frac{x^2}{4T^\gamma} \tag{157}$$

and

$$\beta = T^\gamma. \tag{158}$$

To evaluate this integral we first write

$$e^{-\beta\omega} = \sum_{k=0}^{\infty} \frac{(-\beta)^k}{k!}\omega^k \tag{159}$$

and

$$e^{-\frac{\theta}{\omega}} = H_{1,1}^{1,0}\left[\frac{\theta}{\omega}\,\middle|\,\begin{matrix}-\\(0,1)\end{matrix}\right] \tag{160}$$

so that

$$V_{II}(X,T) = \frac{1}{4\pi T^\gamma}\sum_{k=0}^{\infty}\frac{(-\beta)^k}{k!}\int_0^\infty \omega^{k-\frac{1}{2}} H_{1,1}^{1,0}\left[\frac{\theta}{\omega}\,\middle|\,\begin{matrix}-\\(0,1)\end{matrix}\right] H_{1,1}^{1,0}\left[\omega\,\middle|\,\begin{matrix}(1-\gamma,\gamma)\\(0,1)\end{matrix}\right] d\omega \tag{161}$$

The integral is a convolution integral of the form (171) and this simplifies to

$$V_{II}(X,T) = \frac{1}{4\pi T^\gamma}\sum_{k=0}^{\infty}\frac{(-\beta)^k}{k!} H_{1,2}^{2,0}\left[\theta\,\middle|\,\begin{matrix}\left(1-\frac{\gamma}{2}+\gamma k,\gamma\right)\\(0,1)\left(\frac{1}{2}+k,1\right)\end{matrix}\right] \tag{162}$$

which recovers the result in (46) with $\gamma = \kappa$ and β and ω defined as above.

B Useful Identities

Here we list some useful identities involving the Fox function. Full details can be found in [46, 22].
The fractional derivative of a Fox function is given by

$$\frac{\partial^\nu}{\partial z^\nu}\left\{z^\alpha H_{p,q}^{m,n}\left[(az)^\beta\,\middle|\,\begin{matrix}(a_p,\alpha_p)\\(b_q,\beta_q)\end{matrix}\right]\right\} = z^{\alpha-\nu}H_{p+1,q+1}^{m,n+1}\left[(az)^\beta\,\middle|\,\begin{matrix}(-\alpha,\beta) & (a_p,\alpha_p)\\(b_q,\beta_q) & (\nu-\alpha,\beta)\end{matrix}\right], \tag{163}$$

for $\beta > 0$ and

$$\frac{\partial^\nu}{\partial z^\nu}\left\{z^\alpha H_{p,q}^{m,n}\left[(az)^\beta\,\middle|\,\begin{matrix}(a_p,\alpha_p)\\(b_q,\beta_q)\end{matrix}\right]\right\} = z^{\alpha-\nu}H_{p+1,q+1}^{m+1,n}\left[(az)^\beta\,\middle|\,\begin{matrix}(a_p,\alpha_p) & (1+\alpha-\nu,-\beta)\\(1+\alpha,-\beta) & (b_q,\beta_q)\end{matrix}\right] \tag{164}$$

for $\beta < 0$.
For $c > 0$

$$H_{p,q}^{m,n}\left[x\,\middle|\,\begin{matrix}(a_p,\alpha_p)\\(b_q,\beta_q)\end{matrix}\right] = cH_{p,q}^{m,n}\left[x^c\,\middle|\,\begin{matrix}(a_p,c\alpha_p)\\(b_q,c\beta_q)\end{matrix}\right]. \tag{165}$$

$$H_{p+1,q+1}^{m,n+1}\left[x\,\middle|\,\begin{matrix}(0,\alpha) & (a_p,\alpha_p)\\(b_q,\beta_q) & (r,\alpha)\end{matrix}\right] = (-1)^r H_{p+1,q+1}^{m+1,n}\left[x\,\middle|\,\begin{matrix}(a_p,\alpha_p) & (0,\alpha)\\(r,\alpha) & (b_q,\beta_q)\end{matrix}\right] \tag{166}$$

$$x^\sigma H_{p,q}^{m,n}\left[x\,\middle|\,\begin{matrix}(a_p,\alpha_p)\\(b_q,\beta_q)\end{matrix}\right] = H_{p,q}^{m,n}\left[x\,\middle|\,\begin{matrix}(a_p+\sigma\alpha_p,\alpha_p)\\(b_q+\sigma\beta_q,\beta_q)\end{matrix}\right] \tag{167}$$

Reduction formula with $\Delta > 0$

$$H_{p+1,q+1}^{m+1,n}\left[x\,\middle|\,\begin{matrix}(a_p,\alpha_p) & (d,\Delta)\\(d,\Delta) & (b_q,\beta_q)\end{matrix}\right] = H_{p,q}^{m,n}\left[x\,\middle|\,\begin{matrix}(a_p,\alpha_p)\\(b_q,\beta_q)\end{matrix}\right] \tag{168}$$

Laplace transforms of the Fox Function with $\sigma > 0$

$$\mathscr{L}\left\{t^\omega H_{p,q}^{m,n}\left[zt^{-\sigma}\,\middle|\,\begin{matrix}(a_p,\alpha_p)\\(b_q,\beta_q)\end{matrix}\right]\right\}(s) = s^{-\omega-1}H_{p,q+1}^{m+1,n}\left[zs^\sigma\,\middle|\,\begin{matrix}(a_p,\alpha_p)\\(1+\omega,\sigma)\ (b_q,\beta_q)\end{matrix}\right] \tag{169}$$

and

$$\mathscr{L}\left\{t^\omega H_{p,q}^{m,n}\left[zt^{\sigma}\,\middle|\,\begin{matrix}(a_p,\alpha_p)\\(b_q,\beta_q)\end{matrix}\right]\right\}(s) = s^{-\omega-1}H_{p+1,q}^{m,n+1}\left[zs^{-\sigma}\,\middle|\,\begin{matrix}(-\omega,\sigma)\ (a_p,\alpha_p)\\(b_q,\beta_q)\end{matrix}\right]. \tag{170}$$

Convolution integral of two Fox functions [46]

$$\int_0^t x^{\rho-1}(t-x)^{\sigma-1} H_{p,q}^{m,n}\left[zx^{\mu}(t-x)^{\nu}\,\middle|\,\begin{matrix}(a_p,\alpha_p)\\(b_q,\beta_q)\end{matrix}\right] H_{P,Q}^{M,N}\left[ax^{\mu}(t-x)^{\eta}\,\middle|\,\begin{matrix}(c_P,\gamma_P)\\(d_Q,\delta_Q)\end{matrix}\right] dx$$
$$= t^{\rho+\sigma-1}\sum_{h=1}^{M}\sum_{r=0}^{\infty}\frac{(-1)^r a^{\xi_r}}{r!\delta_h} g(\xi_r)\, t^{(u+\eta)\xi_r} H_{p+2,q+1}^{m,n+2}\left[zt^{\mu+\nu}\,\middle|\,\begin{matrix}(1-\rho-u\xi_r,\mu)\,(1-\sigma-\eta\xi_r,\nu)\,(a_p,\alpha_p)\\(b_q,\beta_q)\,(1-\rho-\sigma-[u+\eta]\xi_r,\mu+\nu)\end{matrix}\right] \tag{171}$$

where

$$g(\theta)=\frac{\prod_{j=1,j\neq h}^{M}\Gamma\left(d_j-\delta_j\theta\right)\prod_{j=1}^{N}\Gamma\left(1-c_j+\gamma_j\theta\right)}{\prod_{j=M+1}^{Q}\Gamma\left(1-d_j+\delta_j\theta\right)\prod_{j=N+1}^{P}\Gamma\left(c_j-\gamma_j\theta\right)} \tag{172}$$

and

$$\xi_r=\frac{d_h+r}{\delta_h}. \tag{173}$$

See [46] for restrictions on parameters in the above.